TISSUE ENGINEERING
Volume 13, Number 1, 2007

DOI: 10.1089/ten.2006.0042

Intervertebral Disc Regeneration Using Platelet-Rich Plasma and Biodegradable Gelatin Hydrogel Microspheres

MASATERU NAGAE,[1] TAKUMI IKEDA,[1] YASUO MIKAMI,[1] HITOSHI HASE,[1] HITOSHI OZAWA,[2] KEN-ICHI MATSUDA,[3] HIROTAKA SAKAMOTO,[3] YASUHIKO TABATA,[4] MITSUHIRO KAWATA,[3] and TOSHIKAZU KUBO[1]

ABSTRACT

This study evaluated the regenerative effects of platelet-rich plasma (PRP) for the degenerated intervertebral disc (IVD) *in vivo*. After induction of IVD degeneration in rabbits, we prepared PRP by centrifuging blood obtained from these rabbits. These PRP were injected into the nucleus pulposus (NP) of the degenerated IVDs after impregnation into gelatin hydrogel microspheres that can immobilize PRP growth factors physiochemically and release them in a sustained manner with the degradation of the microspheres. As controls, microspheres impregnated with phosphate-buffered saline (PBS) and PRP without microspheres were similarly injected. Histologically, notable progress in IVD degeneration with time courses was observed in the PBS control, PRP-only, and sham groups. In contrast, progress was remarkably suppressed over the 8-week period in the PRP group. Moreover, in immunohistochemistry, intense immunostaining for proteoglycan in the NP and inner layer of the annulus fibrosus was observed 8 weeks after administration of PRP-impregnated microspheres. Almost all microspheres were indistinct 8 weeks after the injection, and there were no apparent side effects in this study. Our results suggest that the combined administration of PRP and gelatin hydrogel microspheres into the IVD may be a promising therapeutic modality for IVD degeneration.

INTRODUCTION

LOW BACK PAIN is currently a serious problem in industrial countries, with enormous financial and health care costs,[1–3] and intervertebral disc (IVD) degeneration is one of the major causes of the condition.[4,5] The IVD is a functional unit of the spinal column, and consists of the nucleus pulposus (NP) and annulus fibrosus (AF). Because proteoglycans are highly concentrated in the NP and negatively charged, the NP has a swelling pressure with a high concentration of water.[6,7] Meanwhile, the AF has a lamellar structure with collagen fiber bundles.[8] Because of the structural characteristics of the NP and AF, IVDs possess both mobility and stability, and play fundamental roles in load-bearing.[9] The IVD is an avascular tissue, so it has a very limited ability to regenerate itself. It is known that once IVD degeneration has occurred, it then progresses at an accelerated pace.[10] These particular histological characteristics are the major reason why it is extremely difficult to establish a regenerative therapy for IVD degeneration.

Growth factor therapy is one of the promising modalities to regenerate IVD, because several growth factors have been reported to have therapeutic effects on IVD cells *in vitro*.[11–21] Transforming growth factor-β1 (TGF-β1) has

[1]Department of Orthopaedics, Graduate School of Medical Science, Kyoto Prefectural University of Medicine, Kyoto, Japan.
[2]Department of Anatomy and Neurobiology, Nippon Medical School, Tokyo, Japan.
[3]Department of Anatomy and Neurobiology, Graduate School of Medical Science, Kyoto Prefectural University of Medicine, Kyoto, Japan.
[4]Department of Biomaterials, Field of Tissue Engineering, Institute for Frontier Medical Sciences, Kyoto University, Kyoto, Japan.

been reported to have strong effects on IVD cell proliferation[11] and proteoglycan synthesis.[11,13,16] Platelet-derived growth factor (PDGF) was reported to have an anti-apoptotic effect on AF cells.[14] It has been well known that the platelets contain several kinds of growth factors in α-granules, and these growth factors are released and function in wound healing.[22] TGF-β and PDGF have been recognized as the dominant growth factors.[23] Platelet-rich plasma (PRP) is an autologous concentration of platelets in a small volume of plasma, and contains several kinds of autologous growth factors, such as TGF-β1 and PDGF in high concentrations.[24–26]

Considering this backgrounds, we hypothesized that the administration of PRP growth factors into the degenerated IVD *in vivo* would be an effective, convenient, and safe therapeutic modality for IVD degeneration. We applied gelatin hydrogel microspheres as the drug delivery system (DDS), which can immobilize PRP growth factors ionically and release them in a sustained manner *in vivo* as the microsphere degrades. The objective of this study was to investigate the therapeutic effects of the combined administration of PRP and biodegradable gelatin hydrogel microspheres on the degenerated IVD *in vivo*.

MATERIALS AND METHODS

Preparation of gelatin microspheres

A gelatin sample with an isoelectric point of 5.0 (Nitta Gelatin, Osaka, Japan) was extracted from bovine bone (type I collagen) via an alkaline process. Glutaraldehyde (GA), glycine, and other chemicals were purchased from Wako Pure Chemical Industries (Osaka, Japan) and used without further purification.

Gelatin microspheres were prepared through the GA cross-linking of gelatin aqueous solution.[27] Briefly stated, 10 mL of gelatin aqueous solution (10 wt%, preheated to 40°C) was added to 375 mL of olive oil with stirring to obtain a water-in-oil emulsion. The emulsion temperature was decreased to 4°C, and 100 mL of acetone was added to the emulsion, which was stirred for 1 h. The resulting microspheres were collected, placed into 20 mL of aqueous solution containing 25 μL of GA aqueous solution (25 wt%), and stirred at 4°C for 15 h to facilitate cross-linking. The microspheres were agitated in 20 mL of 10 mM aqueous glycine solution containing Tween-80 (0.1%) at 37°C for 1 h to block the residual aldehyde groups on the unreacted GA. The resulting microspheres were finally washed with double-distilled water, freeze-dried, and sterilized with ethylene oxide gas. The water content of the gelatin microspheres was 99 vol% when calculated from the microsphere volume before and after swelling in phosphate-buffered saline (PBS, pH 7.4) for 24 h at 37°C. The diameter of the microspheres in a swollen state in PBS was measured via light microscopy.

Disc degeneration model

All the experiments in this report were approved by the Kyoto Prefectural University of Medicine Experimental Animal Center Committee. A total of 36 male Japanese white rabbits with a mean weight of 2.8 kg were obtained from the Oriental Bio-Service Laboratory (Kyoto, Japan). IVD degeneration was induced in these rabbits as previously described by Okuma *et al.*[28] and Nomura *et al.*[29] Under inhalation anesthesia with 2.5% isoflurane (Abbott Laboratories, North Chicago, IL), the lateroabdominal fur of each rabbit was shaved, and the skin was disinfected with alcohol and providine-iodine. Through an anterolateral approach, L3–4, L4–5, and L5–6 discs were exposed, and a part of the NP (the weight of the NP aspirated ranged from 0.005 to 0.008 g) in L3–4, L4–5, and L5–6 discs were aspirated using a 21-gauge needle on a 10-mL syringe. After aspiration, the fascia and skin were sutured with 3-0 nylon threads. After awakening from anesthesia, the rabbits were kept for 2 weeks in a cage with freedom of movement. These degeneration-induced rabbits were then divided into 4 groups according to the kind of treatment; PRP group ($n = 9$), PBS control group ($n = 9$), PRP-only group ($n = 9$), and sham group ($n = 9$).

Preparation of gelatin hydrogel microspheres incorporating PRP

In the PRP group and PRP-only group, the preparation of PRP was performed 2 weeks after the partial aspiration of NP. Under general anesthesia, as in the partial aspiration of NP, 20 mL of fresh blood was obtained using a syringe containing 2.0 mL of acid citrate dextrose-A solution to prevent coagulation. The whole blood was centrifuged via a centrifugation apparatus (KN70, Kubota, Tokyo, Japan) at 1500 rpm ($250 \times g$) for 10 min. Subsequently, the only plasma fraction was collected and further centrifuged at 3000 rpm ($1000 \times g$) for 10 min to precipitate the platelets. The precipitated platelets at the bottom of the centrifuge tube were collected with 300 μL of its supernatant (platelet-poor plasma) to yield PRP. The platelet count was conducted in the whole blood and PRP (all measurements were performed by FALCO, Japan). Simultaneously, smears of whole blood and PRP were observed via light microscopy after Wright-Giemsa staining. In the PRP group, immediately after the PRP preparation, 60 μL of PRP was dropped onto 3.0 mg of the freeze-dried and sterilized gelatin microspheres, and incubated for 1 h at 37°C to impregnate PRP into the gelatin microspheres. In the PBS control group, a similar procedure, but using PBS without PRP, was performed to prepare PBS-impregnated gelatin microspheres.

Concentrations of growth factors in the PRP and immobilization into the microspheres

To examine the concentrations of growth factors in the PRP, we measured the concentrations of TGF-β1 ($n = 11$)

and PDGF-BB ($n = 11$) in peripheral blood and PRP by an enzyme-linked immunosorbent assay (ELISA) using a TGF-β1 ELISA Kit and PDGF-BB ELISA Kit (R&D Systems, Minneapolis, MN). We also added PBS to the PRP-impregnated gelatin microspheres under exactly the same conditions as for the actual injection, and measured the concentrations of TGF-β1 ($n = 11$) and PDGF-BB ($n = 11$) in PBS outside the microspheres by ELISA after mixing to examine the rate of immobilization of growth factors into the microspheres.

Injection of gelatin hydrogel microspheres

The injection was performed 2 weeks after the partial aspiration of the NP. In the PRP group, the gelatin hydrogel microspheres impregnated with autologous PRP were injected into the degeneration-induced IVDs. The L3–4, L4–5, and L5–6 discs were exposed through a contralateral approach. Then, 180 μL of PBS was added to the prepared PRP-impregnated gelatin microspheres and mixed gently, and 20 μL of the latter was injected using a 27-gauge insulin injector into each degeneration-induced IVD with careful manipulation. In the PBS control group, PBS-impregnated gelatin microspheres were similarly injected. In the PRP-only group, 5 μL of PRP without microspheres added to 15 μL of PBS was similarly injected. In the sham group, only needle puncture was performed.

Histological evaluation

At 2, 4, and 8 weeks after injection, the rabbits in each group ($n = 3$, each time point) were euthanized by intravenous injection of high-dose pentobarbital sodium (120 mg/kg) (Abbott Laboratories). The L3–4, L4–5, and L5–6 discs of each rabbit were removed immediately as vertebral body–disc–vertebral body units. These units were fixed with 4% paraformaldehyde in 0.1 M phosphate buffer at pH 7.4 with 0.2% picric acid for 7 days at 4°C, and decalcified in 0.5 M EDTA at pH 7.5 for 14 days. Then, the discs were cryoprotected in 20% sucrose for 2 days. The discs were embedded in an optimal cutting temperature compound (Sakura Finetek USA, Torrance, CA), and rapidly frozen with powdered dry ice and sectioned at 12 μm in the midsagittal plane on a cryostat (Leica Jung CM 3000, Nussloch, Germany). The sections were stained with hematoxylin and eosin for histological evaluation. The degenerative changes in the NP were graded using the grading scale described by Nomura *et al.*[29]: grade 0, normal structure; grade 1, no proliferative connective tissue but honeycomb appearance of the extracellular matrix; grade 2, as much as 24% of the NP occupied by proliferative connective tissue; grade 3, 25–50% of the NP occupied by proliferative connective tissue; grade 4, more than 50%; and grade 5, complete replacement of the normal architecture by proliferative connective tissue. The degenerative changes in the AF were graded using the grading system described by Nishimura *et al.*[30]: grade 0, normal structure; grade 1, mildly serpentine appearance of the AF with rupture; grade 2, moderately serpentine appearance of the AF with rupture; grade 3, severely serpentine appearance of the AF with mildly reversed contour; grade 4, severely reversed contour; and grade 5, indistinct. All the grading was done in blinded fashion by the orthopaedic resident, who was blinded to the animal treatments.

The grades for the NP and AF were scored from 0 to 5 (0; grade 0, 1; grade 1, 2; grade 2, 3; grade 3, 4; grade 4, 5; grade 5).

Immunohistochemistry for proteoglycan

Immunohistochemistry for proteoglycan was performed on sections 8 weeks after injection. The frozen sections were dried at room temperature and treated with 1% sodium metaperiodate in PBS to eliminate the endogenous peroxidase activity. After several washes with PBS, they were incubated with 10% normal goat serum in PBS for 10 min under microwave irradiation (MI-77, Azumaya, Tokyo, Japan) to prevent nonspecific staining. Then, the sections were incubated with mouse antihuman cartilage proteoglycan monoclonal antibody (Chemicon, Temecula, CA), which reacts with rabbit proteoglycan and recognizes the short peptides substituted with keratan sulfate side chains and within the core protein of proteoglycans, prepared at a dilution of 1:200 in PBS for 20 min under microwave irradiation. After several washes with PBS, the sections were incubated with antimouse immunoglobulin-HRP (DAKO A/S, Profuktionsvej, Denmark) for 10 min under microwave irradiation. After several washes with PBS, the sections were reacted with a solution containing 3′, 3′-diaminobenzidine tetrahydrochloride (DAB; 20 mg) and 20 μL of H_2O_2 in 100 mL of 50 mM Tris-HCl buffer (pH 7.4) until staining was clearly visible. Finally, the sections were counterstained with hematoxylin.

An immunofluorescence examination was also conducted to clarify and confirm the staining for proteoglycan under fluorescent light. The goat antimouse IgG sera labeled with Alexa-488 were used as the secondary antibody, and the sections were observed with a confocal laser scanning microscope (LSM 510, Zeiss, Jena, Germany). In the immunofluorescence examination, images of the NP, inner layer of the AF (IAF), and growth plate (GP; magnification, ×20) were captured under identical conditions, and divided into areas of 10,000 μm^2. The regions without fluttering or peeling in each area per disc were randomly selected and evaluated. All the images were coded and evaluated without knowledge of the experimental group, and the code was not broken until the analysis was complete. The images were converted into black and white, processed under the same threshold, and analyzed using the NIH Image software package. The optical density (OD) of the immunoreactive area was measured and normalized to the OD of the PBS control group using the NIH Image software package. At least 3 regions in each area per animal were selected and

measured ($n = 9$ discs each for the PRP, PBS control, and PRP-only groups).

Ultrastructural observation of NP cells

In the same manner for the injection, PRP-impregnated microspheres were injected into the L3–4, L4–5, and L5–6 discs of the degeneration-induced rabbits ($n = 3$). The L3–4, L4–5, and L5–6 discs were removed at 8 weeks after injection in the same manner as for the histological evaluation. The L3–4, L4–5, and L5–6 discs in normal control rabbits without injection ($n = 3$) were removed similarly to normal controls. Immediately after the removal, each disc was cut transversely, and the NP was quickly removed, cut into small blocks of about 1 mm^3, and fixed for 2 h in 2.5% GA in 0.1 M phosphate buffer (pH 7.2) at 4°C. After the tissues were rinsed with 8% sucrose-containing phosphate buffer, they were postfixed with 1% osmium tetroxide in 0.1 M phosphate buffer for 2 h at 4°C. After dehydration in a graded ethanol series and treatment with propylene oxide, the tissues were embedded in Quetol 812 at 45°C for 1 day, and then at 60°C for 2 days. The embedded tissues were cut with an ultramicrotome (Ultracut E, Reichert-Jung, Heidelberg, Germany), and the ultrathin sections were mounted on nickel grids, stained with 8% uranyl acetate and lead citrate, and washed with distilled water and dried. The sections were observed and photographed via a JEM-1220 transmission electron microscope (JEOL, Tokyo, Japan).

Statistical analysis

The data on platelet counts was analyzed using the Mann-Whitney U test, and the data on histological grading were analyzed using the Mann-Whitney U test and the Kruskal-Wallis test. The data on the immunostained area for proteoglycan were analyzed using Student's t-test. Statistical significance was accepted when the p value was <0.05. All results are expressed as the mean ± standard error of the mean.

RESULTS

Gelatin hydrogel microspheres as a drug delivery system

After the gelatin hydrogel microspheres were prepared, they were examined via light microscopy to confirm their form and size. Uniformly round microspheres, ranging in diameter from 10 to 20 μm in a swollen state in PBS, were observed (Fig. 1).

High concentration of platelets in the PRP

A blood cell count of the whole blood and the PRP prepared was conducted. The purified PRP contained about 35

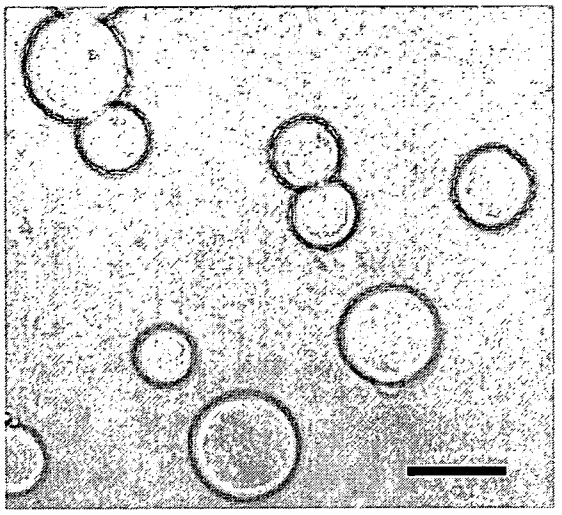

FIG. 1. Photomicrograph of the biodegradable gelatin hydrogel microspheres used as a drug delivery system. Uniformly round microspheres ranging in diameter from 10 to 20 μm in a swollen state in PBS were prepared. Scale bar = 20 μm.

times the number of platelets in the whole blood (35.4 ± 2.1 × 10^4/μL in the whole blood, and 1240.9 ± 86.1 × 10^4/μL in the purified PRP) (Fig. 2A). Examination via light microscopy after Wright-Giemsa staining confirmed that only

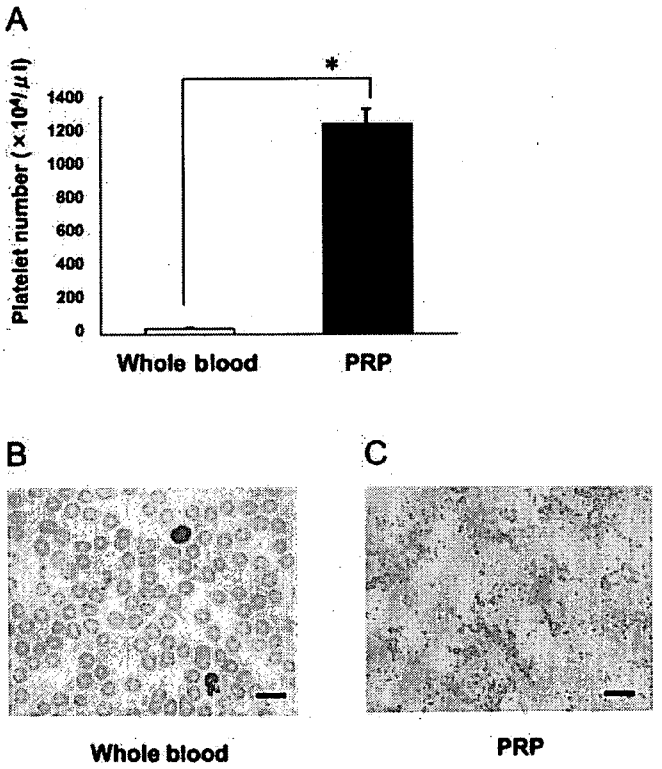

FIG. 2. Concentration of platelets in the platelet-rich plasma (PRP). (**A**) Platelet counts in the whole blood ($n = 9$) and the purified PRP ($n = 9$). The data are expressed as the mean ± standard error of the mean. $p < 0.05$ versus the platelets count in the whole blood. (**B**, **C**) Photomicrographs of whole blood (**B**) and PRP (**C**) stained with Wright-Giemsa stain. Scale bars = 20 μm.

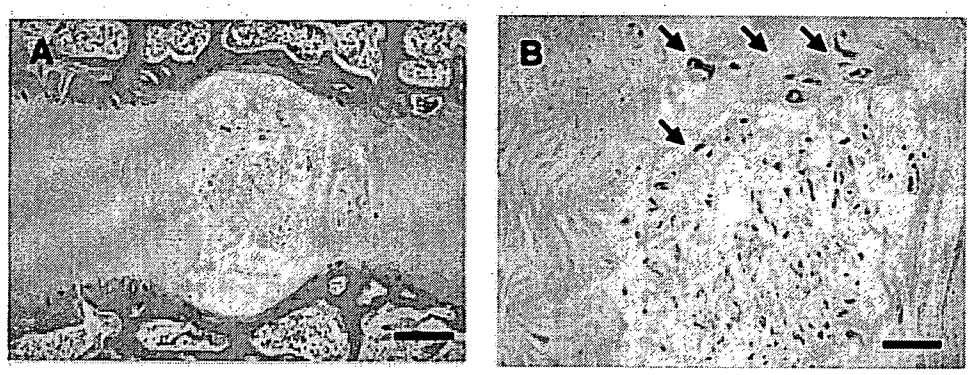

FIG. 3. The histological section of the degeneration-induced disc 2 weeks after the first operation. The irregular arrangement of NP cells and honeycomb appearance of the extracellular matrix in the NP was partially observed. In the AF, a mild serpentine appearance was partially observed. The black arrows indicate the irregular arrangement of NP cells and honeycomb appearance of the extracellular matrix in the NP. Scale bars = 500 μm (**A**) and 200 μm (**B**).

the platelets were highly concentrated, and no other blood cell components were present in the PRP (Fig. 2B, C).

Concentrations of growth factors in the PRP and immobilization into the microspheres

The concentration of TGF-β1 was 71.8 ± 3.2 ng/mL in peripheral blood, and 1653.3 ± 121.3 ng/mL in the PRP. Moreover, the concentration of PDGF-BB was 1.6 ± 0.2 ng/mL in peripheral blood, and 112.9 ± 11.0 ng/mL in the PRP. In the examination of the immobilization of growth factors into microspheres, the outflow to PBS not immobilized in the microspheres was 14.8 ± 2.5% for TGF-β1 (85.6 ± 15.8 ng/mL) and 3.7 ± 0.9% for PDGF-BB (1.4 ± 0.4 ng/mL).

Effect of PRP-impregnated gelatin hydrogel microspheres

To evaluate histologically the effect of PRP on degenerated IVD, midsagittal sections of IVDs from each group stained with hematoxylin and eosin were examined via light microscopy. In the degeneration-induced discs 2 weeks after the first operation, a partial honeycomb appearance of the extracellular matrix in the NP was observed, but no proliferation of connective tissue in the NP was observed. In the AF, a mild serpentine appearance was partially observed (Fig. 3). No significant difference in the degree of degeneration was observed between the L3–4, L4–5, and L5–6 discs.

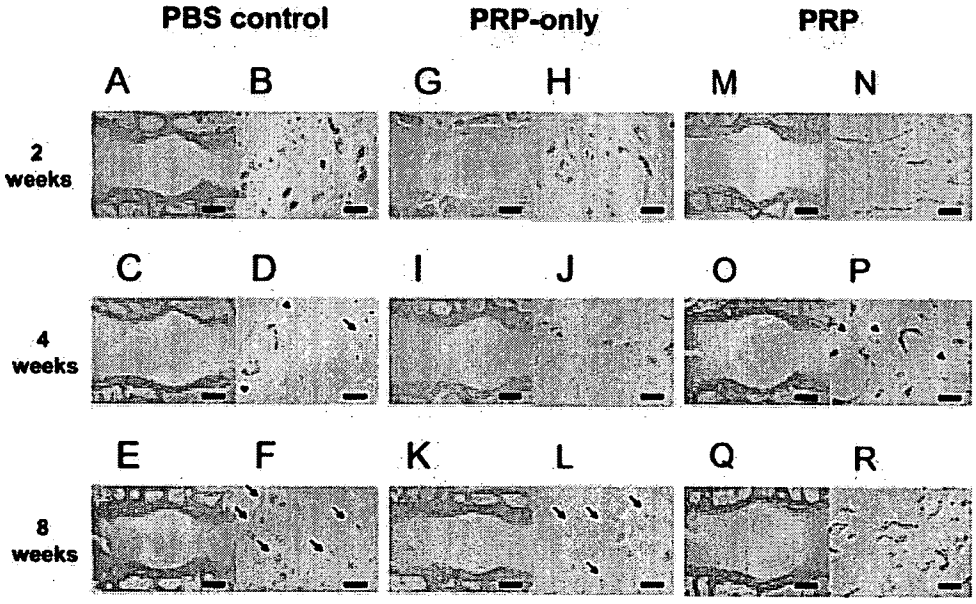

FIG. 4. Histological sections after injection of PBS-impregnated gelatin microspheres (**A, B, C, D, E, F**), PRP-only (**G, H, I, J, K, L**), and PRP-impregnated gelatin microspheres (**M, N, O, P, Q, R**). (**D, F, L**) The black arrows indicate chondrocyte-like cells observed in the proliferative connective tissue. (**D, P**) Arrowheads indicate microspheres at 4 weeks after injection. Scale bars = 700 μm (**A, C, E, G, I, K, M, O, Q**) and 70 μm (**B, D, F, H, J, L, N, P, R**). Stained with hematoxylin and eosin.

In the PBS control, PRP-only, and sham group at 2 weeks after injection, the AF showed a reversed contour in the NP. The distribution of the NP cells became irregular, and the extracellular matrix around the NP cells was heterogeneous and honeycomb-like (Fig. 4A, B, G, H). At 4 weeks after injection, the reversed contour of the AF in the NP was more pronounced and proliferation of connective tissue was also observed. The number of NP cells was notably decreased (Fig. 4C, D, I, J) and chondrocyte-like cells were observed in the connective tissue (Fig. 4D). At 8 weeks after the injection, the NP cells had almost completely disappeared. The lamellar structure in the inner layer of the AF also disappeared, and the NP was completely altered by the proliferated connective tissue (Fig. 4E, F, K, L). Numerous chondrocyte-like cells were observed in the proliferated connective tissue (Fig. 4F, L).

In the PRP group at 2 weeks after the injection, numerous NP cells surrounded by extracellular matrix were observed in the NP, and only mild disruption of the lamellar structure was observed in the AF (Fig. 4M, N). The same histological findings were observed at 4 and 8 weeks after injection, and the structure of both the NP and AF was well maintained during 8 weeks in the PRP group (Fig. 4O–R). In both the PRP group and PBS control group, numerous gelatin hydrogel microspheres were observed in the NP at 2 weeks after injection (Fig. 4B, N), but the number decreased at 4 weeks after injection (Fig. 4D, P). At 8 weeks after injection, almost all of the microspheres were indistinct (Fig. 4F, R). Neither ossification nor invasion of inflammatory cells in the IVD was observed in any group at any time point.

Comparison according to the histological grading scale

To compare the histological findings more clearly, a previously described histological grading scale for the degeneration of the NP[29] and the AF[30] was applied. In scoring grades from 0 to 5, the grade of degeneration in the NP was significantly less severe in the PRP group at 4 and 8 weeks after injection (1.9 ± 0.3 at 2 weeks, 2.1 ± 0.4 at 4 weeks, and 2.4 ± 0.2 at 8 weeks) than in the PBS control group (2.8 ± 0.3, 3.8 ± 0.3, and 4.1 ± 0.4, respectively), PRP-only group (2.8 ± 0.4, 3.9 ± 0.2, and 4.2 ± 0.3, respectively), and sham group (2.4 ± 0.2, 3.2 ± 0.2, and 4.0 ± 0.2, respectively) ($n = 9$ discs at each time point per group) (Fig. 5A). Similarly, the grade of degeneration in AF was significantly less severe in the PRP group at 4 and 8 weeks after injection (2.2 ± 0.3 at 2 weeks, 2.5 ± 0.3 at 4 weeks, and 2.8 ± 0.2 at 8 weeks) than in the PBS control group (3.0 ± 0.3, 3.9 ± 0.2, and 4.3 ± 0.3, respectively), PRP-only group (2.7 ± 0.3, 3.7 ± 0.2, and 4.1 ± 0.3, respectively), and at 8 weeks after injection than in the sham group (2.4 ± 0.2, 3.3 ± 0.3, and 4.0 ± 0.2, respectively) ($n = 9$ discs at each time point per group) (Fig. 5B).

There was no significant difference in the grading score among the groups at 2 weeks after injection in the NP and AF. Statistical analysis of the grading scores for the 3 time points was also performed in NP and AF for each group. As a result, in the NP and AF, a significant difference in the grading score between the 3 time points was observed in the PBS control group, PRP-only group, and sham group, but not in the PRP group. These results suggest that the progress of degeneration in the NP and AF was significantly suppressed in the PRP group as compared to the PBS control group, PRP-only group, and sham group.

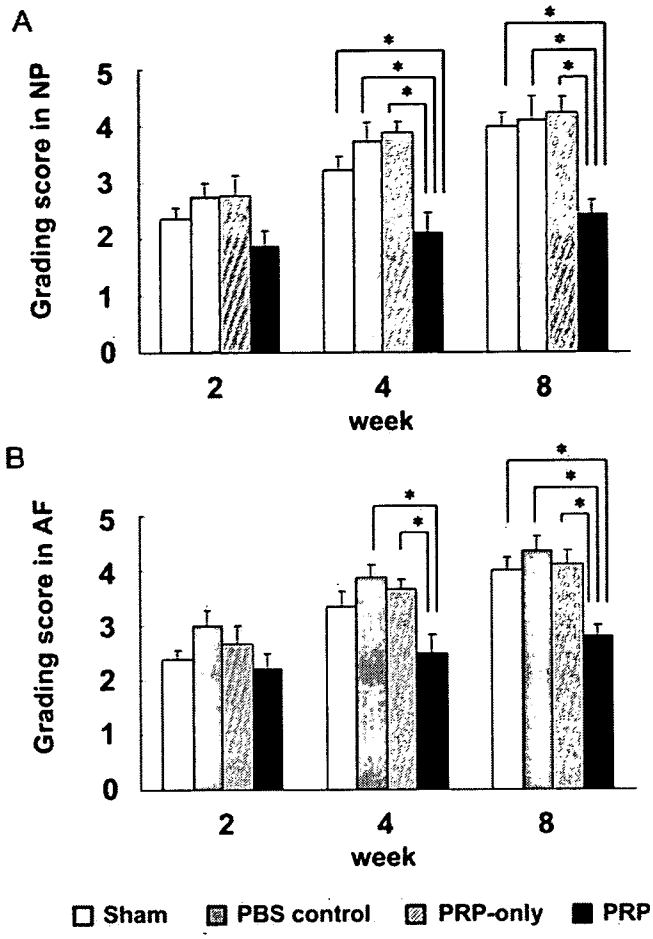

FIG. 5. Evaluation according to the histological grading score. The data are expressed as the mean ± standard error of the mean. Histological grading score in the nucleus pulposus (NP) (**A**) and in the annulus fibrosus (AF) (**B**). $p < 0.05$ versus the score of the PRP group.

High content of proteoglycan after the administration of PRP

To evaluate the effect of PRP for the proteoglycan content after the injection, immunostaining for proteoglycan was conducted. In the PBS control group and the PRP-only group, only weak immunostaining in the NP was observed. Weak immunostaining was also observed around the invaded chondrocyte-like cell (Fig. 6A, B). In the inner layer

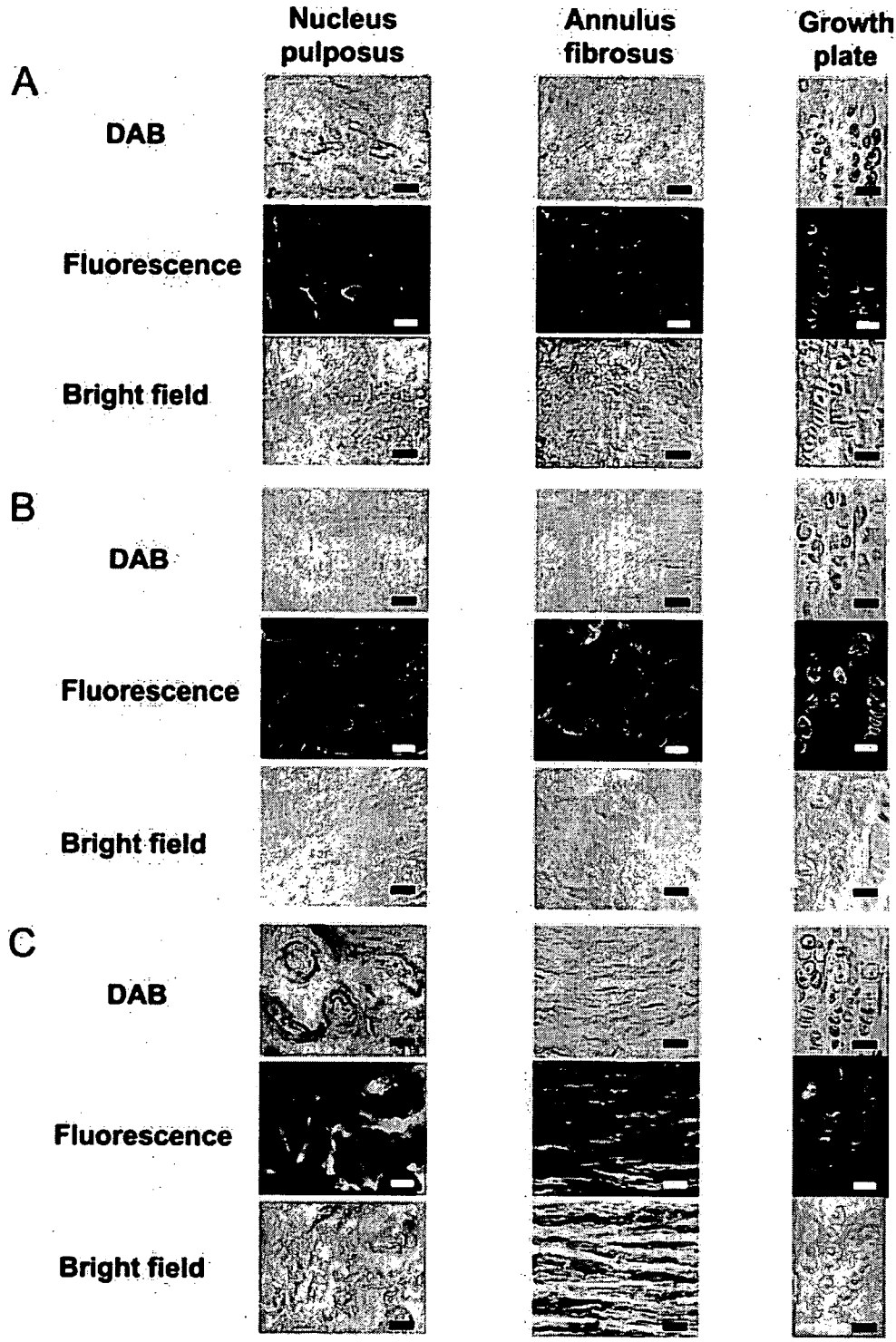

FIG. 6. Immunohistochemical detection for proteoglycan in the PBS control group (**A**), PRP-only group (**B**), and PRP group (**C**). The growth plate was appropriately stained in the PBS control group (**A**), PRP-only group (**B**), and PRP group (**C**). Scale bars = 20 μm.

of the AF with an indistinct lamellar structure, weak and irregular immunostaining was observed (Fig. 6A, B). Otherwise, in the NP of the PRP group, notably intense and regular staining for proteoglycan was observed, and especially intense staining was observed around the NP cells (Fig. 6C). In the inner layer of the AF, regular staining was observed in the lamellar structure (Fig. 6C). No difference in staining for proteoglycan was observed in the chondrocytes of the growth plate among the PBS control group (Fig. 6A), PRP-only group (Fig. 6B), and the PRP group (Fig. 6C).

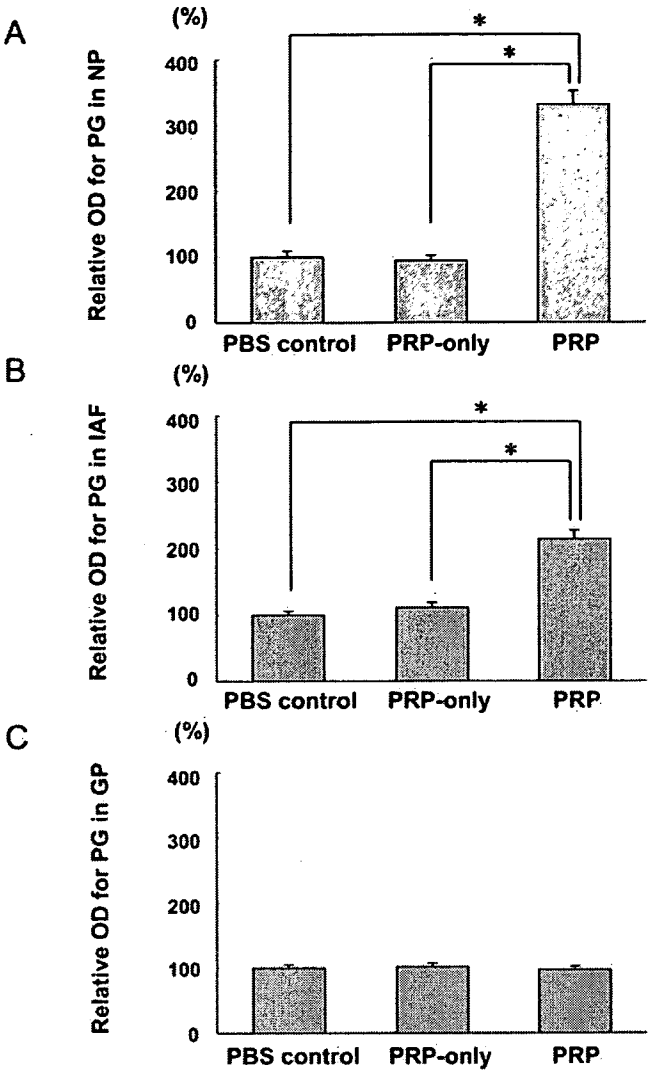

FIG. 7. The calculated optical density (OD) of the immunoreactive area for proteoglycan in the nucleus pulposus (NP) (**A**), inner layer of annulus fibrosus (IAF) (**B**), and growth plate (GP) (**C**). Each value was normalized to the OD of the PBS control group, and expressed as a percentage of the PBS control group value. The data are expressed as the mean ± standard error of the mean. $p < 0.05$ versus the optical density in the PRP group.

Further, in the immunofluorescence examination, the OD of the immunoreactive area for proteoglycan was normalized to the OD of the PBS control group, and expressed as a percentage of the PBS control group value. The relative OD in the PRP group was significantly higher than that in the PBS control group and the PRP-only group in the NP (PBS control group, 100.0 ± 9.1%; PRP-only group, 94.1 ± 7.6%; and PRP group, 331.6 ± 20.7%) (Fig. 7A) and the IAF (100.0 ± 5.9%, 111.2 ± 7.7%, and 213.7 ± 13.4%, respectively) (Fig. 7B). No significant difference was observed in the GP among the 3 groups (100.0 ± 4.9%, 101.9 ± 5.5%, and 97.6 ± 4.9%, respectively) (Fig. 7C).

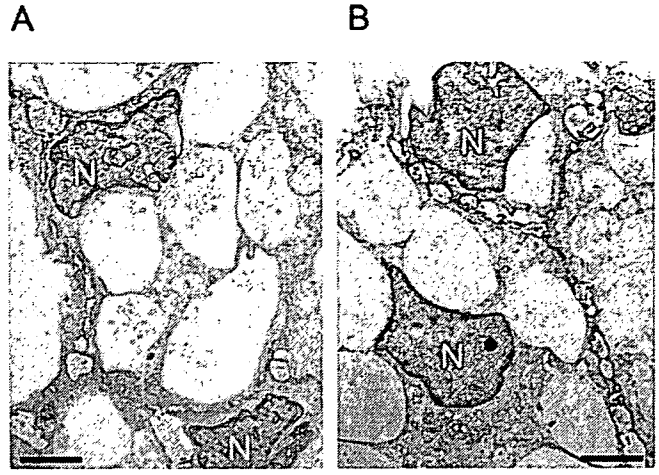

FIG. 8. Transmission electron micrographs of the nucleus pulposus cells in the normal control rabbit intervertebral disc (**A**) and discs 8 weeks after the injection of PRP-impregnated gelatin microspheres (**B**). N, nucleus. Scale bars = 2 μm.

Ultrastructure of NP cells after the administration of PRP

Ultrastructural observation using transmission electron microscopy was conducted. In the normal control NP cells, the nuclei were irregular in shape and enclosed by a well-demarcated nuclear membrane. The nucleoli were observed in the nuclei, and numerous vesicles were observed in the cytoplasm (Fig. 8A). In the NP cells at 8 weeks after the injection of PRP-impregnated gelatin hydrogel microspheres, no apparent ultrastructural difference from the normal control NP cells was observed (Fig. 8B).

DISCUSSION

The present study demonstrates that the combined administration of PRP with gelatin hydrogel microspheres into the NP remarkably suppressed the progress of IVD degeneration. Moreover, there were no apparent side effects such as ossification or inflammation in the IVD and anatomical or physiological changes in NP cells in this study.

PRP is a cocktail of concentrated autologous growth factors, such as TGF-β1 and PDGF, and has been used clinically in the field of oral surgery to promote osteogenesis.[31,32] Safety is one of the advantages of using PRP for tissue regeneration because there is no need for concern about transmissible diseases or immune reactions as PRP is an autologous material.[23] Other advantages include the convenience of preparation and efficacy as a result of the synergistic effects of various endogenous growth factors. However, generally in the application of growth factors *in vivo*, their short biological half-life has been considered a serious drawback.[33,34] Nishida *et al.*[35] reported that the

proteoglycan synthesis in the NP of rabbits was increased by the sustained action of TGF-β1 on transduction of the human TGF-β1 encoding gene into the NP with adenoviral vectors. Walsh *et al.*[36] reported that TGF-β1 had a stimulatory effect on the annular fibrochondrocytes only after administration of multiple injections. These reports suggest the necessity of the sustained action of growth factors in the IVD for regeneration. On the other hand, the therapeutic effects of osteogenic protein-1 (OP-1) for IVD *in vivo* has been reported.[37–39] Masuda *et al.*[39] reported that the single injection of OP-1 into the NP of rabbit worked long term and induced regenerative effects. From these reports, it may be suggested that the necessity of the DDS for IVD regeneration depends on the nature of the growth factors. For the sustained actions of growth factors *in vivo*, either gene transduction or the multiple injection of growth factor into IVD may be impractical for clinical application from the perspective of safety and invasiveness. We considered that an effective, safe, and convenient DDS is desirable for the sustained action of PRP growth factors *in vivo*.

Gelatin has been proved to be a biodegradable and biosafe material, and has been applied clinically as a surgical biomaterial and an ingredient in drugs for a long time. Further, the main component of gelatin is type I collagen, which is a component of normal IVD tissue.[40] We prepared biodegradable gelatin hydrogel microspheres as a carrier of platelet growth factors. One of the main features of this microsphere is its electrical nature.[41] The isoelectric point of gelatin can be changed by the preparation conditions from collagen. We prepared gelatin hydrogel microspheres from acidic gelatin with an isoelectric point of 5.0, which can ionically interact to form a polyion complex with growth factors, such as TGF-β1 and PDGF, with isoelectric points higher than 8.5. Another main feature of this microsphere is its biodegradability, which can be changed by the degree of cross-linking with GA. Tabata *et al.*[41,42] reported that the growth factor immobilized in this hydrogel was released while maintaining its biological activity *in vivo* by the degradation of the hydrogel, and the time course of the release was in close accordance with the rate of hydrogel degradation. The controlled release of growth factors, such as basic fibroblast growth factor,[43] TGF-β1,[44,45] PDGF,[46] and bone morphogenic protein-2,[47] using this gelatin hydrogel system has been reported. Moreover, Hokugo *et al.*[48] reported that this gelatin hydrogel was also a substance capable of activating platelet growth factors such as TGF-β1 and PDGF. From these findings, we were convinced that the gelatin hydrogel microsphere would be an ideal DDS for IVD regeneration using PRP. For biodegradability of gelatin hydrogel microspheres, the water content of the gelatin microspheres we prepared was 99 vol%, when calculated from the microsphere volume before and after swelling in PBS solution (pH 7.4) (data not shown). From the histological finding that almost all microspheres were indistinct at 8 weeks after injection, we considered that our administration of microspheres successfully resulted in the sustained release of the growth factor in IVD for 8 weeks.

We also considered it necessary to impregnate the highly concentrated and purified PRP growth factors into the microspheres for the long-term and efficient release of growth factors in IVDs. We therefore modified the previously reported method of preparing PRP,[49] excluding blood cell components other than the platelets, and prepared a PRP that contained highly concentrated platelets (Fig. 2C). Our experiment using ELISA indicates that TGF-β1 and PDGF-BB were also highly concentrated in the PRP we prepared. It has been recognized that more than 95% of the presynthesized growth factors present in the α-granules of platelets are secreted within 1 h after blood clotting.[22] Therefore, in our preparation of PRP-impregnated gelatin hydrogel microspheres, the PRP was dropped onto the gelatin hydrogel microspheres immediately after preparation and incubated for 1 h at 37°C to secrete growth factors and immobilize it to the gelatin microspheres before injection. Our experiment using ELISA indicates that most of the TGF-β1 and PDGF-BB secreted were immobilized into the gelatin hydrogel microspheres. These results indicate that highly concentrated TGF-β1 and PDGF-BB immobilized in gelatin hydrogel microspheres can be administered into the NP.

We used the IVD degeneration model with partial aspiration of the NP. This model has been recognized for its ability to create reproducible and progressive disc degeneration, and was used in previous studies on disc regeneration.[28–30,50]

Histological observation of the IVD sections 2 weeks after the injection revealed clear differences between the PRP group and the other groups in the NP, although the histological grading score did not reach a significant difference. This indicates that the degeneration of the NP was accelerating in the PBS control, PRP-only, and sham groups, while it was suppressed in the PRP group. In the PRP-only group, similar to the PBS control and sham group, notable progress in degeneration with time courses was observed. In contrast, progress was significantly suppressed over the 8-week period in the PRP group. It is likely that the activation of PRP growth factors was not induced or maintained by the single injection of PRP.

It has been known that proteoglycan plays a major role in the water content and swelling pressure in IVD,[6,51,52] and a decrease of proteoglycan in the NP triggers IVD degeneration.[53–55] Further, in an *in vitro* experiment, it was reported that PRP significantly stimulated the synthesis of proteoglycan and collagen on NP and AF cells.[56,57] In our immunohistological experiment, a significant difference in staining for proteoglycan was observed between the PRP group and the other groups, and intense and regular staining was observed in the PRP group. Considering these results, it may be speculated that the PRP growth factors acted on the NP and IAF cells in a sustained manner, and the synthesis of proteoglycan was upregulated in the PRP group. In addition

to the direct influence on the IVD cells, swelling pressure in the NP might be maintained by the accumulation of proteoglycan, and consequently, the collapse of the AF structure might be suppressed. Although further experiments are required to evaluate the various effects of PRP growth factors such as cell proliferation and the suppression of apoptosis, it may be suggested that the promotion of proteoglycan synthesis plays important roles in IVD regeneration by PRP growth factors *in vivo*.

It has been described that PRP growth factors bind to the transmembrane receptors of target cells, but never enter the cell or its nucleus, and consequently they are not mutagenic.[22] In our observation using transmission electron microscopy, no apparent changes in ultrastructure as compared to normal NP cells were observed in the NP cells after the administration of PRP-impregnated gelatin hydrogel microspheres. This result suggests that no anatomical or physiological change in NP cells was induced by the administration of PRP.

The present study showed histologically the therapeutic effects of PRP-impregnated gelatin hydrogel microspheres for early-stage IVD degeneration, but the therapeutic effects on advanced IVD degeneration and in the long term remain unclear. In addition, it is known that human NP cells in infancy are notochordal NP cells, similar to those of the rabbits we used, but are replaced by chondrocytic NP cells with growth.[58] It is necessary to clarify further the therapeutic effects of PRP growth factors on the advanced IVD degeneration and chondrocytic NP cells. Recently, the usefulness of imaging techniques such as magnetic resonance imaging and radiography for the evaluation of IVD degeneration has been reported.[37,59,60] Further evaluation using these imaging techniques may make clear the various effects of PRP growth factors *in vivo*.

To our knowledge, this is the first report of the administration of PRP into degenerated IVDs *in vivo*. Considering the results, it is suggested that the combined administration of PRP growth factors with gelatin hydrogel microspheres into the NP, is an effective, safe, and convenient method, and may be an innovative and promising therapeutic modality for IVD degeneration.

ACKNOWLEDGMENTS

The authors thank Drs. Joji Mochida and Daisuke Sakai (Department of Orthopaedic Surgery, Functional Reconstruction, Tokai University School of Medicine) for technical assistance. This work was supported by Grants- in-Aid for Scientific Research from the Ministry of Education, Science, Sports, Culture and Technology, Japan.

REFERENCES

1. Waddell, G. Low back pain: a twentieth century health care enigma. Spine **21,** 2820, 1996.
2. Williams, D.A., Feuerstein, M., Durbin, D., and Pezzullo, J. Health care and indemnity costs across the natural history of disability in occupational low back pain. Spine **23,** 2329, 1998.
3. Ekman, M., Johnell, O., and Lidgren, L. The economic cost of low back pain in Sweden in 2001. Acta Orthop. **76,** 275, 2005.
4. Andersson, G.B. Epidemiological features of chronic low-back pain. Lancet **354,** 581, 1999.
5. Biyani, A., and Andersson, G.B. Low back pain: pathophysiology and management. J. Am. Acad. Orthop. Surg. **12,** 106, 2004.
6. Urban, J.P., and McMullin, J.F. Swelling pressure of the lumbar intervertebral discs: influence of age, spinal level, composition, and degeneration. Spine **13,** 179, 1988.
7. Johnstone, B., Urban, J.P., Roberts, S., and Menage, J. The fluid content of the human intervertebral disc. Comparison between fluid content and swelling pressure profiles of discs removed at surgery and those taken postmortem. Spine **17,** 412, 1992.
8. Marchand, F., and Ahmed, A.M. Investigation of the laminate structure of lumbar disc annulus fibrosus. Spine **15,** 402, 1990.
9. Humzah, M.D., and Soames, R.W. Human intervertebral disc: structure and function. Anat. Rec. **220,** 337, 1988.
10. Lipson, S.J., and Muir, H. Experimental intervertebral disc degeneration: morphologic and proteoglycan changes over time. Arthritis Rheum. **24,** 12, 1981.
11. Thompson, J.P., Oegema, T.R. Jr., and Bradford, D.S. Stimulation of mature canine intervertebral disc by growth factors. Spine **16,** 253, 1991.
12. Osada, R., Ohshima, H., Ishihara, H., Yudoh, K., Sakai, K., Matsui, H., and Tsuji, H. Autocrine/paracrine mechanism of insulin-like growth factor-1 secretion, and the effect of insulin-like growth factor-1 on proteoglycan synthesis in bovine intervertebral discs. J. Orthop. Res. **14,** 690, 1996.
13. Gruber, H.E., Fisher, E.C. Jr., Desai, B., Stasky, A.A., Hoelscher, G., and Hanley, E.N. Jr. Human intervertebral disc cells from the annulus: three-dimensional culture in agarose or alginate and responsiveness to TGF-beta1. Exp. Cell. Res. **235,** 13, 1997.
14. Gruber, H.E., Norton, H.J., and Hanley, E.N. Jr. Anti-apoptotic effects of IGF-1 and PDGF on human intervertebral disc cells *in vitro*. Spine **25,** 2153, 2000.
15. Takegami, K., Thonar, E.J., An, H.S., Kamada, H., and Masuda, K. Osteogenic protein-1 enhances matrix replenishment by intervertebral disc cells previously exposed to interleukin-1. Spine **27,** 1318, 2002.
16. Alini, M., Li, W., Markovic, P., Aebi, M., Spiro, R.C., and Roughley, P.J. The potential and limitations of a cell-seeded collagen/hyaluronan scaffold to engineer an intervertebral disc-like matrix. Spine **28,** 446, 2003.
17. Kim, D.J., Moon, S.H., Kim, H., Kwon, U.H., Park, M.S., Han, K.J., Hahn, S.B., and Lee, H.M. Bone morphogenetic protein-2 facilitates expression of chondrogenic, not osteogenic, phenotype of human intervertebral disc cells. Spine **28,** 2679, 2003.
18. Masuda, K., Takegami, K., An, H., Kumano, F., Chiba, K., Andersson, G.B., Schmid, T., and Thonar, E. Recombinant osteogenic protein-1 upregulates extracellular matrix metabolism

by rabbit annulus fibrosus and nucleus pulposus cells cultured in alginate beads. J. Orthop. Res. **21,** 922, 2003.
19. Risbud, M.V., Izzo, M.W., Adams, C.S., Arnold, W.W., Hillibrand, A.S., Vresilovic, E.J., Vaccaro, A.R., Albert, T.J., and Shapiro, I.M. An organ culture system for the study of the nucleus pulposus: description of the system and evaluation of the cells. Spine **28,** 2652, 2003.
20. Yoon, S.T., Kim, K.S., Li, J., Park, J.S., Akamaru, T., Elmer, W.A., and Hutton, W.C. The effect of bone morphogenetic protein-2 on rat intervertebral disc cells *in vitro*. Spine **28,** 1773, 2003.
21. Takegami, K., An, H.S., Kumano, F., Chiba, K., Thonar, E.J., Singh, K., and Masuda, K. Osteogenic protein-1 is most effective in stimulating nucleus pulposus and annulus fibrosus cells to repair their matrix after chondroitinase ABC-induced *in vitro* chemonucleolysis. Spine J. **5,** 231, 2005.
22. Marx, R.E. Platelet-rich plasma: evidence to support its use. J. Oral Maxillofac. Surg. **62,** 489, 2004.
23. Marx, R.E., Carlson, E.R., Eichstaedt, R.M., Schimmele, S.R., Strauss, J.E., and Georgeff, K.R. Platelet-rich plasma: growth factor enhancement for bone grafts. Oral Surg. Oral Med. Oral Pathol. Oral Radiol. Endod. **85,** 638, 1998.
24. Weibrich, G., Kleis, W.K., Hafner, G., and Hitzler, W.E. Growth factor levels in platelet-rich plasma and correlations with donor age, sex, and platelet count. J. Craniomaxillofac. Surg. **30,** 97, 2002.
25. Okuda, K., Kawase, T., Momose, M., Murata, M., Saito, Y., Suzuki, H., Wolff, L.F., and Yoshie, H. Platelet-rich plasma contains high levels of platelet-derived growth factor and transforming growth factor-beta and modulates the proliferation of periodontally related cells *in vitro*. J. Periodontol. **74,** 849, 2003.
26. Eppley, B.L., Woodell, J.E., and Higgins, J. Platelet quantification and growth factor analysis from platelet-rich plasma: implications for wound healing. Plast. Reconstr. Surg. **114,** 1502, 2004.
27. Tabata, Y., Hijikata, S., Muniruzzaman, M., and Ikada, Y. Neovascularization effect of biodegradable gelatin microspheres incorporating basic fibroblast growth factor. J. Biomater. Sci. Polym. Ed. **10,** 79, 1999.
28. Okuma, M., Mochida, J., Nishimura, K., Sakabe, K., and Seiki, K. Reinsertion of stimulated nucleus pulposus cells retards intervertebral disc degeneration: an *in vitro* and *in vivo* experimental study. J. Orthop. Res. **18,** 988, 2000.
29. Nomura, T., Mochida, J., Okuma, M., Nishimura, K., and Sakabe, K. Nucleus pulposus allograft retards intervertebral disc degeneration. Clin. Orthop. Relat. Res. **389,** 94, 2001.
30. Nishimura, K., and Mochida, J. Percutaneous reinsertion of the nucleus pulposus. An experimental study. Spine **23,** 1531, 1998.
31. Mazor, Z., Peleg, M., Garg, A.K., and Luboshitz, J. Platelet-rich plasma for bone graft enhancement in sinus floor augmentation with simultaneous implant placement: patient series study. Implant Dent. **13,** 65, 2004.
32. Oyama, T., Nishimoto, S., Tsugawa, T., and Shimizu, F. Efficacy of platelet-rich plasma in alveolar bone grafting. J. Oral Maxillofac. Surg. **62,** 555, 2004.
33. Puolakkainen, P.A., Twardzik, D.R., Ranchalis, J.E., Pankey, S.C., Reed, M.J., and Gombotz, W.R. The enhancement in wound healing by transforming growth factor-beta 1 (TGF-beta1) depends on the topical delivery system. J. Surg. Res. **58,** 321, 1995.
34. Lee, S.J. Cytokine delivery and tissue engineering. Yonsei Med J. **41,** 704, 2000.
35. Nishida, K., Kang, J.D., Gilbertson, L.G., Moon, S.H., Suh, J.K., Vogt, M.T., Robbins, P.D., and Evans, C.H. Modulation of the biologic activity of the rabbit intervertebral disc by gene therapy: an *in vivo* study of adenovirus-mediated transfer of the human transforming growth factor beta 1 encoding gene. Spine **24,** 2419, 1999.
36. Walsh, A.J., Bradford, D.S., and Lotz, J.C. *In vivo* growth factor treatment of degenerated intervertebral discs. Spine **29,** 156, 2004.
37. An, H.S., Takegami, K., Kamada, H., Nguyen, C.M., Thonar, E.J., Singh, K., Andersson, G.B., and Masuda, K. Intradiscal administration of osteogenic protein-1 increases intervertebral disc height and proteoglycan content in the nucleus pulposus in normal adolescent rabbits. Spine **30,** 25, 2005.
38. Kawakami, M., Matsumoto, T., Hashizume, H., Kuribayashi, K., Chubinskaya, S., and Yoshida, M. Osteogenic protein-1 (osteogenic protein-1/bone morphogenetic protein-7) inhibits degeneration and pain-related behavior induced by chronically compressed nucleus pulposus in the rat. Spine **30,** 1933, 2005.
39. Masuda, K., Imai, Y., Okuma, M., Muehleman, C., Nakagawa, K., Akeda, K., Thonar, E., Andersson, G., and An, H. S. Osteogenic protein-1 injection into a degenerated disc induces the restoration of disc height and structural changes in the rabbit annular puncture model. Spine **31,** 742, 2006.
40. Roberts, S., Menage, J., Duance, V., Wotton, S., and Ayad, S. 1991 Volvo Award in basic sciences. Collagen types around the cells of the intervertebral disc and cartilage end plate: an immunolocalization study. Spine **16,** 1030, 1991.
41. Tabata, Y., and Ikada, Y. Protein release from gelatin matrices. Adv. Drug Deliv. Rev. **31,** 287, 1998.
42. Tabata, Y., Nagano, A., and Ikada, Y. Biodegradation of hydrogel carrier incorporating fibroblast growth factor. Tissue Eng. **5,** 127, 1999.
43. Ozeki, M., and Tabata, Y. Promoted growth of murine hair follicles through controlled release of basic fibroblast growth factor. Tissue Eng. **8,** 359, 2002.
44. Yamamoto, M., Tabata, Y., Hong, L., Miyamoto, S., Hashimoto, N., and Ikada, Y. Bone regeneration by transforming growth factor beta1 released from a biodegradable hydrogel. J. Control. Release **64,** 133, 2000.
45. Hong, L., Tabata, Y., Miyamoto, S., Yamamoto, M., Yamada, K., Hashimoto, N., and Ikada, Y. Bone regeneration at rabbit skull defects treated with transforming growth factor-beta1 incorporated into hydrogels with different levels of biodegradability. J. Neurosurg. **92,** 315, 2000.
46. Kanematsu, A., Yamamoto, S., Ozeki, M., Noguchi, T., Kanatani, I., Ogawa, O., and Tabata, Y. Collagenous matrices as release carriers of exogenous growth factors. Biomaterials **25,** 4513, 2004.
47. Yamamoto, M., Takahashi, Y., and Tabata, Y. Controlled release by biodegradable hydrogels enhances the ectopic bone formation of bone morphogenetic protein. Biomaterials **24,** 4375, 2003.
48. Hokugo, A., Ozeki, M., Kawakami, O., Sugimoto, K., Mushimoto, K., Morita, S., and Tabata, Y. Augmented bone

regeneration activity of platelet-rich plasma by biodegradable gelatin hydrogel. Tissue Eng. **11,** 1224, 2005.
49. Yazawa, M., Ogata, H., Nakajima, T., Mori, T., Watanabe, N., and Handa, M. Basic studies on the clinical applications of platelet-rich plasma. Cell Transplant. **12,** 509, 2003.
50. Sakai, D., Mochida, J., Yamamoto, Y., Nomura, T., Okuma, M., Nishimura, K., Nakai, T., Ando, K., and Hotta, T. Transplantation of mesenchymal stem cells embedded in Atelocollagen gel to the intervertebral disc: a potential therapeutic model for disc degeneration. Biomaterials **24,** 3531, 2003.
51. Urban, J.P., and McMullin, J.F. Swelling pressure of the intervertebral disc: influence of proteoglycan and collagen contents. Biorheology **22,** 145, 1985.
52. Ohshima, H., Tsuji, H., Hirano, N., Ishihara, H., Katoh, Y., and Yamada, H. Water diffusion pathway, swelling pressure, and biomechanical properties of the intervertebral disc during compression load. Spine **14,** 1234, 1989.
53. Pearce, R.H., Grimmer, B.J., and Adams, M.E. Degeneration and the chemical composition of the human lumbar intervertebral disc. J. Orthop. Res. **5,** 198, 1987.
54. Roughley, P.J., Alini, M., and Antoniou, J. The role of proteoglycans in aging, degeneration and repair of the intervertebral disc. Biochem. Soc. Trans. **30,** 869, 2002.
55. Oegema, T.R. Jr. Biochemistry of the intervertebral disc. Clin. Sports Med. **12,** 419, 1993.
56. Masuda, K., Oegema, T.R. Jr., and An, H.S. Growth factors and treatment of intervertebral disc degeneration. Spine **29,** 2757, 2004.
57. Akeda, K., An, H.S., Pichika, R., Attawia, M., Thonar, E.J., Lenz, M.E., Uchida, A., and Masuda, K. Platelet-rich plasma (PRP) stimulates the extracellular matrix metabolism of porcine nucleus pulposus and anulus fibrosus cells cultured in alginate beads. Spine **31,** 959, 2006.
58. Trout, J.J., Buckwalter, J.A., Moore, K.C., and Landas, S.K. Ultrastructure of the human intervertebral disc. I. Changes in notochordal cells with age. Tissue Cell **14,** 359, 1982.
59. Sobajima, S., Kompel, J.F., Kim, J.S., Wallach, C.J., Robertson, D.D., Vogt, M. T., Kang, J.D., and Gilbertson, L.G. A slowly progressive and reproducible animal model of intervertebral disc degeneration characterized by MRI, X-ray, and histology. Spine **30,** 15, 2005.
60. Kim, K.S., Yoon, S.T., Li, J., Park, J.S., and Hutton, W.C. Disc degeneration in the rabbit: a biochemical and radiological comparison between four disc injury models. Spine **30,** 33, 2005.

Address reprint requests to:
Masateru Nagae
Department of Orthopaedics
Graduate School of Medical Science
Kyoto Prefectural University of Medicine
Kajiicho 465, Kawaramachi-Hirokoji, Kamigyo-ku
Kyoto 602-8566
Japan

E-mail: sho-gun@koto.kpu-m.ac.jp

Available online at www.sciencedirect.com
ScienceDirect
Journal of Controlled Release 118 (2007) 169–176
journal of controlled release
www.elsevier.com/locate/jconrel

Controlled-release of epidermal growth factor from cationized gelatin hydrogel enhances corneal epithelial wound healing

Kuniko Hori [a,*], Chie Sotozono [a], Junji Hamuro [a], Kenta Yamasaki [a], Yu Kimura [b], Makoto Ozeki [b], Yasuhiko Tabata [b], Shigeru Kinoshita [a]

[a] *Department of Ophthalmology, Kyoto Prefectural University of Medicine, Hirokoji, Kawaramachi, Kamigyoku, Kyoto 602-0841, Japan*
[b] *Department of Biomaterials, Institute for Frontier Medical Sciences, Kyoto University, Kyoto, Japan*

Received 12 August 2006; accepted 5 December 2006
Available online 16 December 2006

Abstract

We designed a new ophthalmic drug-delivery system for epidermal growth factor (EGF) from the biodegradable hydrogel of cationized gelatin. We placed a cationized gelatin hydrogel (CGH) with incorporated ^{125}I-labelled EGF in the conjunctival sac of mice and measured the residual radioactivity at different times to evaluate the *in vivo* profile of EGF release. Approximately 60–67% and 10–12% of EGF applied initially remained 1 and 7 days after application, respectively; whereas EGF delivered in topically applied solution or via EGF impregnation of soft contact lenses disappeared within the first day. We also placed CGH films with 5.0 μg of incorporated EGF on round corneal defects in rabbits to evaluate the healing process using image analysis software and to assess epithelial proliferation immunohistochemically by counting the number of Ki67-positive cells. The application of a CGH film with incorporated EGF resulted in a reduction in the epithelial defect in rabbit corneas accompanied by significantly enhanced epithelial proliferation compared with the reduction seen after the topical application of EGF solution or the placement of an EGF-free CGH film. The controlled release of EGF from a CGH placed over a corneal epithelial defect accelerated ocular surface wound healing.

Keywords: Controlled release; Corneal wound healing; Epidermal growth factor; Cationized gelatin hydrogel; Hydrogel degradation

1. Introduction

Growth factors (GF) are relevant bioactive proteins that play a vital role in regulating cell functions and maintaining tissue homeostasis; a wide variety of GF are involved in the wound-healing process of the ocular surface [1,2]. An enormous number of studies have revealed that topical treatment with GF, such as epidermal growth factor (EGF) [3–7], keratinocyte growth factor [8], acidic and basic fibroblast growth factor [9,10], and nerve growth factor [11] enhanced the wound-healing effect in primate models and in clinical trials, suggesting promising therapeutic efficacy of GF in ocular surface diseases. As these findings elucidated more extensively the clinical usefulness of GF, a system to deliver protein drugs has become more and more needed. Compared to conventional synthetic low molecular weight drugs, proteins are more unstable during their storage and administration, and they are susceptible to denaturation during the drug formulation process [12–14].

This has hampered the ocular therapeutic application of GF, and eye drops, the simplest formulation for ophthalmic administration, have remained the standard mode of drug delivery. However, rapid pre-corneal loss requires the frequent instillation of highly concentrated drug solutions to achieve drug contact with the cornea for periods long enough to obtain therapeutic efficacy [15–17]. To overcome the low bioavailability of drugs in conventional eye drops, various drug delivery systems have been explored. Viscous vehicles such as ointments and polymeric hydrogels improve drug bioavailability moderately [15–19]. Hydrogel soft contact lenses (SCL) [20–23] have been used as a pre-corneal drug reservoir system and collagen shields [24–26] have been studied as an alternative to provide higher and sustained drug concentrations for up to several hours. As available drug delivery systems focused on the delivery of low molecular weight drugs rather than protein drugs, we set out to design a finely tuned system to deliver GF to the ocular surface.

* Corresponding author. Tel.: +81 75 251 5577; fax: +81 75 251 5663.
E-mail address: khori@ophth.kpu-m.ac.jp (K. Hori).

0168-3659/$ - see front matter © 2007 Elsevier B.V. All rights reserved.
doi:10.1016/j.jconrel.2006.12.011

We previously explored the use of biodegradable gelatin hydrogels for the controlled release of GF [27–29] and succeeded in enhancing the *in vivo* biological activity of GF in angiogenesis [30,31], osteogenesis [32,33], and adipogenesis [34]. From the release system, biologically active GF were released as a result of biodegradation of hydrogel as the release carrier.

In the current study we investigated whether the gelatin hydrogel could be used for the controlled release of GF by examining the release profiles of GF incorporated into the gelatin hydrogel and accelerated ocular surface wound-healing effect. Because it enhances epithelial wound healing [3–7], we used EGF as a representative GF. We prepared anionized and cationized derivatives of acidic- and basic-type gelatins, respectively, and various hydrogels by cross-linking gelatin samples. We then impregnated the hydrogels with EGF to obtain the hydrogel incorporating EGF and examined the *in vitro* and *in vivo* EGF release profiles. To evaluate their therapeutic efficacy, we applied the hydrogel incorporating EGF to rabbit corneal epithelial defects, measured the decrease in the size of the defects, and quantified epithelial proliferation by counting the number of Ki67-positive cells.

2. Materials and methods

2.1. Preparation of gelatin derivatives

Gelatin was chemically derivatized by introducing functional groups into acidic-and basic-type gelatin (isoionic point (IIP) 5.0 and 9.0, Nitta Gelatin Co., Osaka, Japan) to obtain anionized or cationized gelatin derivatives, respectively. For anionization, succinic anhydride was conjugated to the amino groups of acidic gelatin side-residues to obtain a succinylated derivative of gelatin [35]. For another anionization, 2.606 g of sulfoacetic acid (5 ml) were added to 45 ml of 4 wt.% acidic-type gelatin solution in phosphate-buffered saline (PBS); then the pH was adjusted to 5.0. After adding 1-ethyl-3-(3-dimethylaminopropyl) carbodiimide hydrochloride, the reaction was continued at 37 °C for 18 h; this was followed by dialyzing against milli-Q purified water for 48 h at room temperature (RT). The dialyzed solution was freeze-dried to obtain a sulfoethylated gelatin derivative. For cationization, various amounts of ethylenediamine were conjugated to the amino groups of basic gelatin side-residues to obtain cationized gelatin (CG) [36–38]. The CG was named according to the molar ratio of ethylenediamine added to the carboxyl groups of gelatin (E0, E0.5, E3, E10, and E50). Using the 2,4,6-trinitrobenzene sulfonate (TNBS) method [39], the percent introduced for each derivative was calculated as the percentage increase or decrease of the amino groups in cationized or anionized gelatins. The IIP of the derivatives was measured by the JIS PAGI method [40]. Briefly, 1 wt.% of gelatin derivative solution was passed through ion exchange column (cationic (DOWEX 50W-X8) and anionic (DOWEX 1-X8) exchange resins were mixed) at 40 °C and the pH of the elution was measured with pH meter (HORIBA D-22) at 40 °C.

2.2. Preparation of gelatin hydrogels

2.2.1. Preparation of freeze-dried gelatin hydrogel blocks and SCL

The gelatin hydrogel blocks were prepared by chemical cross-linking of gelatin [35,38]. The freeze-dried gelatin hydrogels were cut into blocks of 2.0 and 1.0 mg for *in vitro* and *in vivo* release experiments, respectively. Commercially available SCL (Precision UV®) were rinsed 3 times with milli-Q, freeze-dried, and cut into 4.0- and 2.0-mg blocks.

2.2.2. Preparation of thin CG hydrogel (CGH) films

Thin CGH films were prepared by air-drying and dehydrothermal cross-linking of CGH. Aqueous solutions of 5 wt.% CG (1000 μl for mouse — and 250 μl for rabbit experiments) were cast into $2 \times 2\text{-cm}^2$ molds, air-dried at 4 °C, and then cross-linked in a vacuum oven at 160 °C for 54 h. The resulting CGH films (0.025 mm in thickness) were cut into 2.0-mg pieces for the mouse experiments; they were punched out with a trephine to obtain 9-mm round pieces for the rabbit experiments.

2.2.3. Measurement of gelatin hydrogel water content

The water content of the gelatin hydrogel (weight ratio of water in the hydrogel to the wet hydrogel) was calculated from the hydrogel weight before and after 24-h swelling in milli-Q at 37 °C [35].

2.3. Estimation of in vitro EGF release

Human recombinant EGF (PeproTech EC Ltd., London, UK) was radiolabelled using the chloramine-T method [41]. After dropping 10 μl of ^{125}I-labeled EGF solution onto freeze-dried gelatin hydrogel blocks and SCL, they were left overnight at 4 °C to obtain gelatin hydrogels and SCL with incorporated ^{125}I-labeled EGF (^{125}I-EGF-gelatin hydrogels, ^{125}I-EGF–SCL). They were then agitated at 37 °C in 1 ml of PBS. The PBS supernatant was removed and replaced at 30, 60, 120, and 360 min or at 24 and 48 h with an identical volume of fresh PBS solution. The radioactivity in each supernatant was measured on a gamma counter (ARC-301B, Aloka, Tokyo, Japan) to obtain the EGF release profiles over time ($n=3$, at each time point).

2.4. Animal experiments

All animal experiments were in compliance with the ARVO Statement for the Use of Animals in Ophthalmic and Vision Research; all experimental procedures were pre-approved by the Committee for Animal Research of Kyoto Prefectural University of Medicine and Kyoto University. We used 5-6-week-old female ddY mice in our *in vivo* EGF release and CGH degradation experiments and female Japanese white rabbits, each weighing 1.5–2.0 kg, in the wound-healing experiments.

2.5. Estimation of in vivo EGF release

We used radiolabelled EGF to obtain the *in vivo* EGF release profiles in the conjunctival sac of mice. The animals were

Table 1
Preparation of hydrogels from gelatin derivatives

Code		Gelatin concentration (wt.%)	Reagent concentration (mg/ml)	Percent introduced (mol/mol%)	Isoionic point	The water content of hydrogels (wt.%)
A	Acidic-type gelatin	10	1.25	–	5.05	90.1
SE	Sulfoethylated gelatin	10	1.00	26.5	4.57	97.4
S	Succinylated gelatin	10	1.25	21.1	4.72	87.9
B	Basic-type gelatin	10	1.25	–	8.81	87.7
E0.5	Cationized gelatin	10	0.62	14.1	10.01	94.7
E3	Cationized gelatin	10	0.93	24.2	9.06	96.5
E10	Cationized gelatin	10	0.93	33.9	8.94	97.7
E25	Cationized gelatin	10	0.93	45.6	8.14	94.6
E50	Cationized gelatin	10	0.93	45.1	7.84	84.5

anesthetized with an intraperitoneal injection of Nembutal (Dainippon sumitomo pharma, Osaka, Japan). After introducing ^{125}I-EGF–CGH (E0.5 and E3) into the conjunctival sac of mice we performed tarsorrhaphy. At 1, 3, 5, and 7 days after treatment, the remaining hydrogel and surrounding ocular tissue were excised and the residual radioactivity was measured (n=4, for each time point). The ratio of the remaining radioactivity to the introduced radioactivity was expressed in terms of % remaining radioactivity and the time-profiles of remaining radioactivity were compared with the profiles of ^{125}I-EGF–SCL and the profiles obtained after the single topical application of ^{125}I-labeled EGF solution.

2.6. Estimation of in vivo degradation of CGH

The *in vivo* time profiles of CGH (carrier alone) degradation were examined using E0.5 and E3 CGH radiolabelled with ^{125}I-Bolton-Hunter reagent [42]. ^{125}I-CGH were placed in the conjunctival sac of mice and the degradation profiles were assessed as above (n=4, for each time point).

2.7. Evaluation of enhanced wound healing

To determine the effect of controlled EGF release on wound healing we used a rabbit corneal epithelial defect model. Japanese white rabbits were anesthetized by an intramuscular injection of ketamine hydrochloride (Daiichi-Sankyo, Co., Ltd., Tokyo, Japan) and xylazine hydrochloride (Bayer Medical Ltd., Tokyo, Japan). Oxybuprocaine hydrochloride (Santen Pharmaceutical Co., Ltd., Osaka, Japan) was instilled topically. After creating a round corneal epithelial defect (177 mm^2) in the center of the cornea by superficial keratectomy with a 7.5-mm trephine, the cornea was overlaid with a thin CGH film that incorporated 5.0 μg of EGF (0.11 mm in thickness), a SCL (0.14 mm in thickness) was sutured with 10-0 nylon over the film to keep it in place, and then tarsorrhaphy was performed. To evaluate wound healing, the area of the defect was measured 48 and 96 h later using image analysis software (Scion Image) (n=7 for each time point). The healing profiles of defects covered with EGF–CGH film, EGF-free-CGH film, or treated with the single application of topical EGF solution were compared. In control experiments, an aqueous solution of 5.0 μg EGF was applied topically to the defect and 2 h later a CGH film was placed on the cornea; the defect in other rabbits was covered with an EGF-free CGH film. As in the experimental groups, an SCL was sutured over the film with 10-0 nylon sutures and this was followed by tarsorrhaphy.

2.8. Immunohistochemical assessment of corneal epithelial proliferation

Epithelial proliferation was assessed immunohistochemically by counting the number of Ki67-positive cells. At 48 h after wounding, the eyes were excised (n=6 for each experimental group) and 6 μm-thick cryostat sections of corneo–scleral tissue were cut and processed for Ki67 immunostaining using monoclonal mouse anti-human Ki67 antigen (Dako Cytomation, Glostrup, Denmark). The sections were fixed with zamboni, incubated for 1 h at RT with an anti-Ki67 antibody (1:75 dilution) and for 2 h at RT with Alexa Fluor 488-conjugated goat anti-mouse IgG (Invitrogen, Carlsbad, CA., USA) (1:2000 dilution), mounted in fluorescent mounting media, and then examined under a fluorescence microscope (AX70, OLYMPUS, Tokyo, Japan) equipped with a CCD camera.

The total number of Ki67-positive cells in each section was counted in an area extending from 1 mm outside the limbocorneal junction to the leading edge of the regenerated epithelium (total area). Cell counts were also obtained in 3 different 1-mm wide zones in the leading edge and inside and outside the limbocorneal junction (leading edge, periphery, and limbus, respectively). The proliferation profiles obtained after a single application of topical EGF solution and after EGF-free CGH film placement were compared.

2.9. Statistical analysis

All results were expressed as the mean±standard deviation of the mean. For statistical analysis we used the Tukey–Kramer post-test for multiple comparisons. Differences were considered significant at $p<0.05$.

3. Results

3.1. Preparation and characterization of gelatin hydrogels

As EGF-carrier candidates, we prepared 2 kinds of anionized and 5 kinds of cationized gelatin derivatives from acidic- and

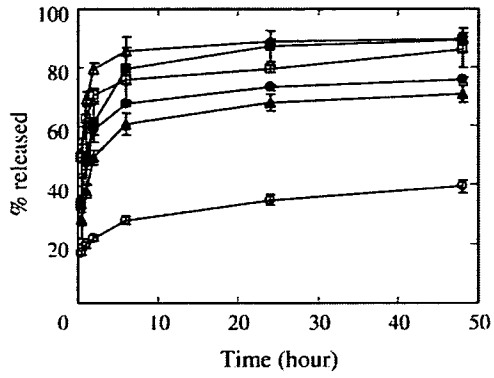

Fig. 1. Time course of the *in vitro* release of EGF from different gelatin hydrogels in PBS at 37 °C. The hydrogels were impregnated with ^{125}I-labeled EGF solution. E0.5 CGH (○), SE (Δ), S (□), B (●), and A (▲). ■ indicates the profile of EGF release from commercially available SCL.

basic-type gelatin, respectively (Table 1). IIP measurements revealed that the reaction produced anionized and cationized gelatin derivatives. For cationized gelatin, the % ethylenediamine introduced increased with the increase in the amount of ethylenediamine added initially. Irrespective of the gelatin type, hydrogels were prepared by chemical cross-linking of the gelatin with glutaraldehyde.

3.2. *In vitro release profiles of EGF from gelatin hydrogels*

Because the gelatin used as the EGF carrier in controlled-release experiments must be able to interact physicochemically with EGF, we first assessed the *in vitro* EGF release profiles in our candidate gelatin hydrogels. As shown in Fig. 1, the release profiles were biphasic; there was an initial burst in release and this was followed by a no-release phase. The E0.5 CGH showed an initial release-burst of less than 25% of the incorporated EGF; approximately 70% of the EGF was retained thereafter. On the other hand, approximately 60–80% of incorporated EGF was released initially from other gelatin hydrogels and SCL. This finding indicates that CGH interacts with EGF, resulting in a suppressed EGF release under *in vitro* conditions in which the hydrogel is not degraded.

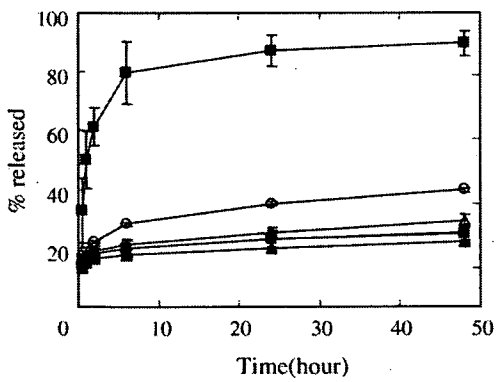

Fig. 2. Time course of the *in vitro* release of EGF from CGH cationized at different extents in PBS at 37 C. The hydrogels were prepared by impregnating CGH with ^{125}I-labeled EGF solution. E0.5 (○), E3 (Δ), E10 (□), E25 (●), and E50 (▲). ■ indicates the profile of EGF release from commercially available SCL.

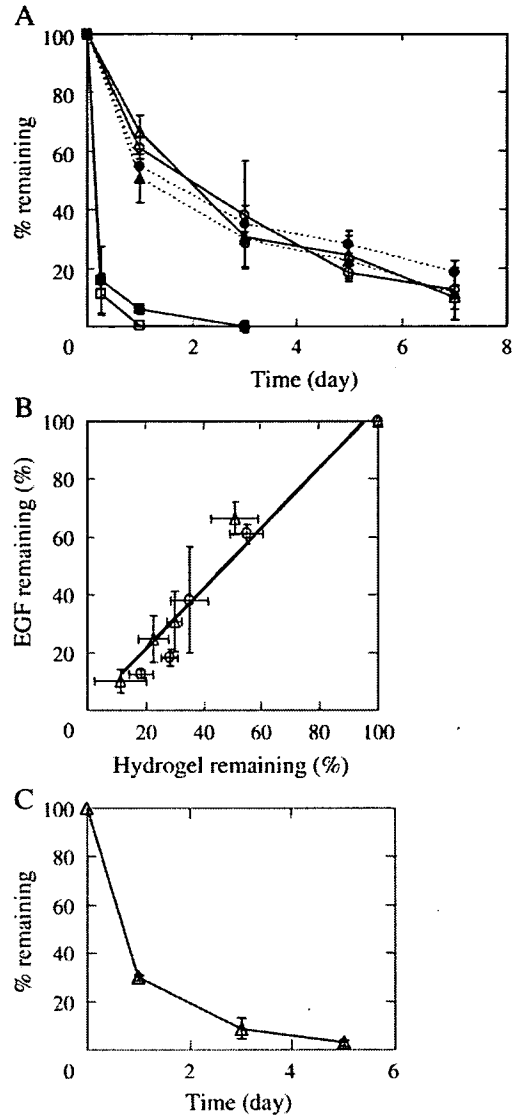

Fig. 3. *In vivo* release profile of EGF from CGH. A. Time course of radioactivity remaining after the application of CGH with incorporated ^{125}I-labeled EGF (open symbols) and ^{125}I-labeled CGH (carrier alone) (closed symbols) into the conjunctival sac of mice. E0.5 (○, ●) and E3 (Δ, ▲) CGHs. □ and ■ indicate the time-course of radioactivity remaining after the application of topical ^{125}I-labeled EGF solution and of SCL with incorporated ^{125}I-labeled EGF, respectively. B. Radioactivity remaining after the application of CGH with incorporated ^{125}I-labelled EGF as a function of remaining radioactivity after the application of ^{125}I-labeled CGHs. E0.5 (○), E3 CGHs (Δ). The correlation coefficient was $R=0.98$. C. Time-course of radioactivity after the application of a thin CGH film, prepared by dehydrothermal cross-linking, with incorporated ^{125}I-labeled EGF into the conjunctival sac of mice.

3.3. *In vitro profiles of EGF release from CGH*

To preserve the original nature of gelatin, the extent of cationization should be minimized. As shown in Fig. 2, the *in vitro* release profiles of EGF from E0.5-E50 CGH were also biphasic. All examined CGH showed an initial EGF release-burst of 45%; more than 55% of the incorporated EGF was retained thereafter. Although the amount of EGF released in the initial burst tended to increase as the extent of gelatin cationization decreased, the level of cationization appeared to have no significant effect on the EGF release profile over time.

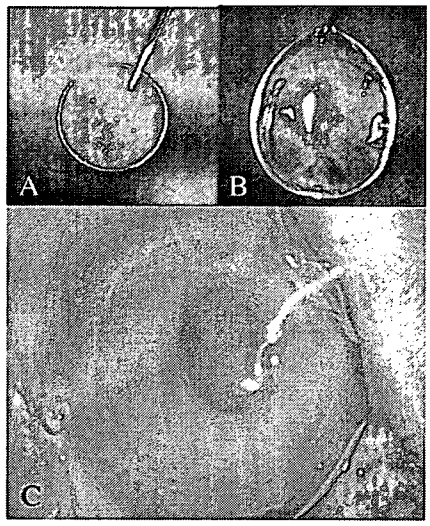

Fig. 4. Slit lamp microscopy of CGH film. A. Dried thin CGH film prepared by dehydrothermal cross-linking. B. Rehydrated thin CGH film on a SCL. C. A thin, transparent CGH film was applied to the rabbit corneal defect subsequently covered with a SCL.

The degree of cationization required for sustained EGF retention was as small as E0.5 or E3.

3.4. *In vivo profiles of EGF release from CGH*

Using radiolabelled EGF, we determined the *in vivo* time profile of EGF release from CGH in the conjunctival sac of mice (Fig. 3A). When EGF was delivered in an eye drop solution, the radioactivity disappeared from the ocular tissue within the first day. A similar trend was observed when we applied SCL with incorporated EGF; only 5.8% of EGF remained in the SCL on the day after placement. On the other hand, in E0.5 and E3 EGF–CGH, the residual radioactivity of EGF on day 1 was 60.9 and 66.4%, respectively; these levels gradually decreased to12.5% and 10.0%, respectively, on day 7. These observations indicate that EGF was retained in the CGH and released to the ocular surface in a sustained manner over a 7-day period.

To determine whether the EGF release is the result of degradation of the carrier hydrogel, we performed *in vivo* degradation tests in the conjunctival sac of mice. The residual radioactivity in E0.5 and E3 carrier gels was 54.7% and 50.7%, respectively, on day 1; 18.4% and 11.2%, respectively, remained on day 7. The radioactivity decrease pattern was similar to that of radiolabelled EGF incorporated into CGH. As shown in Fig. 3B, there was a good linear correlation between the radioactivity remaining in ^{125}I-labelled EGF and ^{125}I-labelled CGH; the correlation coefficient was 0.98. This observation suggests that EGF incorporated into CGH was released in a controlled manner onto the ocular surface as a result of biodegradation of the carrier hydrogel.

We also examined the pattern of EGF release from the E3 CGH film, prepared for application over the rabbit corneal defect by dehydrothermal cross-linking. As shown in Fig. 3C, the film released EGF for 5 days into the conjunctival sac of mice. The residual radioactivity of EGF incorporated into the film was 29.8% on day 1 and 2.85% on day 5, demonstrating that while the release of EGF was gradual, it was faster than from CGH prepared by chemical cross-linking.

3.5. *Epithelial wound healing*

We used a rabbit corneal epithelial defect model to assess the wound-healing effect of the controlled release of EGF from CGH. The CGH film applied to the rabbit cornea was thin and optically transparent (Fig. 4); it retained its shape for 3–4 days after placement. As shown in Fig. 5, fluorescein slit lamp microscopic study of representative corneal defects at 0, 48, and 96 h showed that the original size of the defect (177 mm^2) was

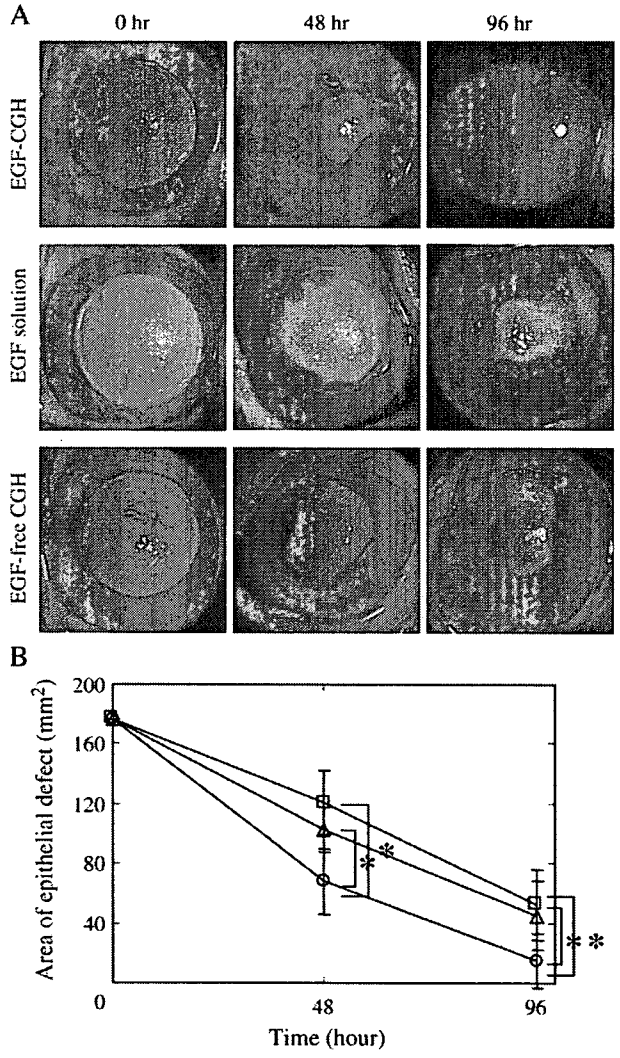

Fig. 5. Enhanced wound healing in a rabbit corneal epithelial defect model. A. Fluorescein slit lamp micrograph of a representative corneal defect obtained 0, 48, and 96 h after the application of a CGH film with incorporated EGF (upper), EGF solution (middle), and an EGF-free CGH film (lower). B. Time-course of the closure of a corneal epithelial defect after the application of a CGH film with incorporated EGF (○), EGF solution (△), and an EGF-free CGH film (□). *$p<0.05$, significantly different from the control at the corresponding time point (Tukey–Kramer post-test).

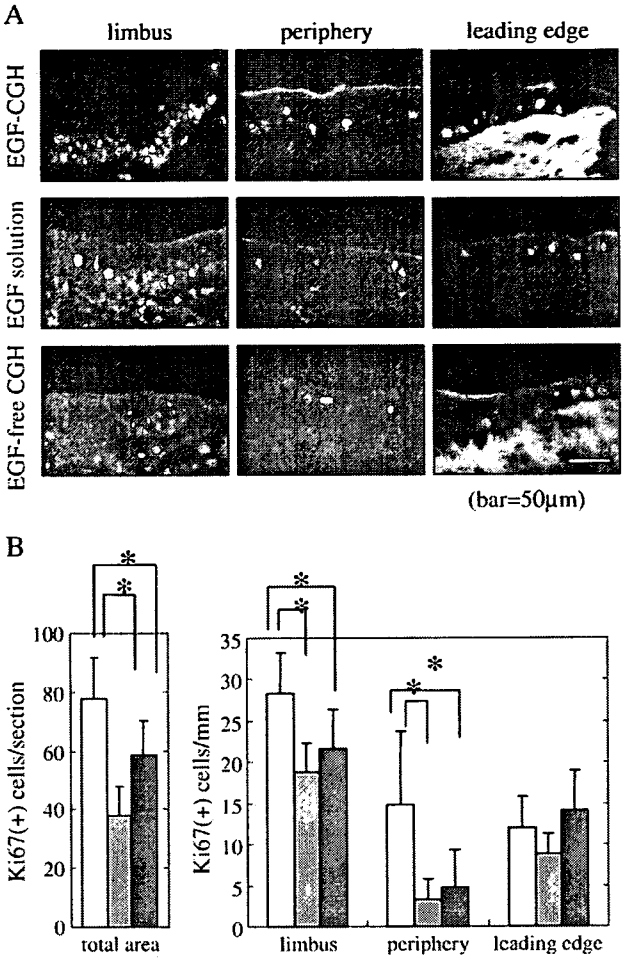

Fig. 6. Immunohistochemical evaluation of corneal epithelial proliferation. A. Fluorescein micrograph of a representative section used for the counting of Ki67-positive cells at 48 h after the application of a CGH film with incorporated EGF (upper), EGF solution (middle), or an EGF-free CGH film (lower). The section is from regenerated corneal epithelium at the site of the epithelial defect. B. Ki67-positive epithelial cell counts at the site of the epithelial defect after the application of a CGH film with incorporated EGF (white bars), EGF solution (grey bars), and an EGF-free CGH film (black bars). The Ki67-positive cell counts were obtained in whole regenerated epithelium in each section (total area) and at 3 different 1-mm-zones, i.e. the limbus, periphery, and leading edge of the epithelium. (*$p<0.05$, Tukey–Kramer post-test).

reduced to 68.0±22.2 mm^2 at 48 and to 15.3±18.2 mm^2 at 96 h after wounding, respectively. At 48 and 96 h, placement of the EGF–CGH film resulted in significantly greater wound healing than did placement of the EGF-free CGH film (120.8±21.8 and 52.2±23.5 mm^2, respectively) or the topical application of EGF solution (102.4±13.8 and 42.0±23.0 mm^2, respectively).

3.6. Histological evaluation of corneal epithelial defects

By counting the number of Ki67-positive cells at 48 h after wounding we further assessed the wound-healing effect of the controlled release of EGF from CGH (Fig. 6). The number of Ki67-positive cells was significantly greater after the application of EGF–CGH than EGF-free CGH film (77.5±13.8 vs. 58.5±11.9) or the administration of EGF solution (38.0±10.0). The Ki67-positive cell counts in the 3 different 1-mm zones we examined (leading edge, periphery, and limbus) were also higher in corneas treated with the EGF–CGH film than the EGF-free CGH film or the EGF solution; this increase appeared to be localized to the limbus where the numbers were 28.3±4.93 vs. 18.7±3.60 and 22.0±5.53 and the periphery (14.7±9.00 vs. 3.29±2.55 and 4.81±4.49). In the leading edge, the number of Ki67-positive cells was comparable (11.9±4.03, 8.9±2.44, and 14.1±4.79, respectively). These results indicate that the controlled release of EGF increased epithelial proliferation until 48 h after wounding especially in the peripheral cornea and resulted in accelerated wound closure.

4. Discussion

We developed a system that uses a biodegradable CGH as the carrier to deliver GF to the ocular surface. The application of CGH with incorporated EGF prolonged the EGF release and led to accelerated wound healing in a rabbit corneal epithelial defect model.

EGF, a soluble protein that is found in various bodily fluids, can stimulate the proliferation of epithelial cells, fibroblasts, and other cell types. Endogenous EGF plays a key role in regulating the normal turnover and replacement of corneal epithelial cells and in constitutive corneal wound healing. It is mainly secreted by the lacrimal gland and while it is abundant in the tears of healthy subjects [43], the EGF concentration was significantly reduced in the tears of patients with chronic epithelial defects [44].

The efficacy of EGF for treating human ocular surface diseases has been studied since the 1970s and the enhancement of corneal epithelial proliferation by exogenous EGF has been examined in animal models [3,45] and clinical trials [5,6]. In most earlier studies, EGF was administered 4–5 times a day in the form of topical eye drops [3,45] and yet its bioavailability was probably low. Sheardown et al. who used a Morgan therapeutic lens found that the continuous exposure to low EGF concentrations increased the corneal epithelial healing rate [46]; they also reported the Carbopol polymeric gel as a clinically acceptable means of delivering EGF continuously [47]. Polymeric gel-mediated delivery systems have been found to prolong the corneal contact time due to their viscosity [48,49], and they have been used in other animal studies [50,51]. However, the drug retention time is limited to several hours because the polymeric gels are diluted, become dispersed, and the drugs drain into the nasolacrimal duct due to high tear–fluid turnover.

The drug delivery system introduced here is advantageous because it offers a much more prolonged period of GF release, than conventional delivery systems based on diffusion-dependent release. In diffusion-dependent drug release systems, the drugs are passively desorbed in an initial burst and washed out. In degradation-dependent drug release systems, on the other hand, the gelatin hydrogels binds GF by physicochemical interactions and releases the protein drug slowly only when it is biodegraded.

In degradation-dependent drug release systems, the carrier must 1) interact with peptide drugs by polyionic complexation and 2) biodegrade at the site of its introduction. For the first requirement, we found that among the 9 kinds of gelatin

hydrogels we examined, CGH was a carrier that interacted physicochemically with EGF. Analysis by isoelectric focusing showed the isoelectric point of EGF to be 4.5 [52]. As CG is a positively charged gelatin derivative, the 2 proteins were able to interact electrostatically. Our previous study reveled that CGH did not exhibit cytotoxicity when applied to cells cultured *in vitro* (data not shown) or inflammatory reactions when implanted in the muscle tissue of mice [38].

As for the second requirement, in the current study we examined the *in vivo* release of EGF incorporated in CGH upon its degradation in the conjunctival sac of mice. The release of GF is regulated by the water content of the hydrogel, the drug amount, and the proteolytic activity at the site of application. The water content is a measure of hydrogel degradation period. The hydrogels with a higher water content degraded faster and released GF sooner. The water content of E0.5 and E3 CGH was 94.7% and 96.5%, respectively, and the hydrogels degraded gradually in the course of 7 days, with concomitant release of EGF. On the ocular surface, nonspecific proteolytic or hydrolytic enzymes in the tear fluid may be involved in gelatin hydrogel degradation. As microenvironmental conditions affect local enzymatic activity, in the presence of intense inflammation, for example, degradation tends to be accelerated.

When we examined the ability of SCL, a representative conventional reservoir system, to retain EGF *in vitro* and *in vivo*, we found that SCL did not retain EGF for sufficiently long periods to allow for its controlled release (Figs. 1–3). We also detected no interactions between EGF and acidic- and basic-type I collagen *in vitro* (data not shown).

Another relevant issue to be addressed on the gelatin hydrogel release system is the improved stability of GFs. By forming a drug-carrier complex such as our CGH system, GF in the carrier matrix retain their bioactivity because they are protected against proteolytic and other denaturation processes after *in vivo* application. Complex formation can be achieved by simply dropping the drug solution onto the dried gelatin hydrogels, eliminating the need for potentially damaging pharmacological processes. With the exception of the method reported by Kim et al. [53] who used cyclodextrin and poloxamer gel, drug delivery and release systems reported so far failed to improve the stability of EGF.

In our rabbit corneal epithelial defect model we documented accelerated wound healing after the application of CGH with the ability for sustained EGF release (Fig. 5). The time course of narrowing of epithelial defect area is a standard measure to evaluate the corneal epithelial healing process [3,8]. EGF released from CGH triggered the accelerated epithelial wound closure, to a significantly greater extent than did the topical application of EGF solution, which suggest our CGH system, successfully released biologically active EGF for extended period. In addition, for corneas treated with the EGF–CGH, no unusual clouding or neovascularization was observed, as was reported in the corneas treated with frequent instillations of EGF solution [3].

In the rabbit experiment, the thin CGH film was created by dehydrothermal — rather than chemical cross-linking, because our CGH film is superior in its transparency to hydrogels obtained by chemical cross-linking as shown in Fig. 4. The water content of the CGH film was 89.9% and EGF was released over a period of 5 days in the conjunctival sac of mice. The water content of the CGH film was lower, but the EGF release faster, than in the chemically cross-linked gelatins used in the first two mice experiments. However, despite its ophthalmologically essential transparency, the CGH film is not practical for use in the clinical setting. To keep it in place, it had to be covered with a SCL sutured to the conjunctiva. In addition, CGH films with a water content below 90% simulated foreign bodies on the cornea and interfered with re-epithelialization (data not shown) and the prolonged presence of the film may lead to hypoxic sequelae. For the clinical applications, the film should be of a laminate type consisting of contact lens and gelatin film with a high oxygen permeability.

Our immunohistochemical analysis showed that the application of EGF–CGH film resulted in accelerated epithelial proliferation especially in the peripheral cornea. This observation coincides with findings that EGF enhanced corneal epithelial wound healing via the increased proliferation [3] or migration of epithelial cells [54]. Our group previously reported that at 48 h after corneal wounding, the frequent instillation of EGF solution increased epithelial proliferation almost two-fold and that endogenously up-regulated proliferation was most vigorous in the cornea applied with vehicle only [3]. Our present data suggest that the controlled release of EGF continued to accelerate epithelial proliferation until 48 h after wounding and that it was comparable or superior to the frequent instillation of EGF solution, especially in the peripheral cornea.

The biochemical nature of gelatins can be modified by derivatization procedures other than the ones used here. Theoretically, our delivery system can be adapted to other GF and soluble factors and gelatin hydrogels can be produced in forms other than discs and thin films to accommodate the site of application.

Although further studies are underway to assess the clinical applicability of the drug-release system introduced here, the use of gelatin hydrogels for the sustained delivery of ophthalmic drugs opens new possibilities for the treatment of patients with ocular surface diseases.

References

[1] J. Imanishi, K. Kamiyama, I. Iguchi, M. Kita, C. Sotozono, S. Kinoshita, Growth factors: importance in wound healing and maintenance of transparency of the cornea, Prog. Retin. Eye Res. 19 (1) (2000) 113–129.
[2] B. Klenkler, H. Sheardown, Growth factors in the anterior segment: role in tissue maintenance, wound healing and ocular pathology, Exp. Eye Res. 79 (5) (2004) 677–688.
[3] T. Kitazawa, S. Kinoshita, K. Fujita, K. Araki, H. Watanabe, Y. Ohashi, R. Manabe, The mechanism of accelerated corneal epithelial healing by human epidermal growth factor, Invest. Ophthalmol. Vis. Sci. 31 (9) (1990) 1773–1778.
[4] S. Kinoshita, Clinical application of epidermal growth factor in ocular surface disorders, J. Dermatol. 19 (11) (1992) 680–683.
[5] S. Daniele, L. Frati, C. Fiore, G. Santoni, The effect of the epidermal growth factor (EGF) on the corneal epithelium in humans, Albrecht von Graefes Arch. Klin. Exp. Ophthalmol. 210 (3) (1979) 159–165.
[6] J.C. Pastor, M. Calonge, Epidermal growth factor and corneal wound healing. A multicenter study, Cornea 11 (4) (1992) 311–314.
[7] C. Scardovi, G.P. De Felice, A. Gazzaniga, Epidermal growth factor in the topical treatment of traumatic corneal ulcers, Ophthalmologica 206 (3) (1993) 119–124.

[8] C. Sotozono, T. Inatomi, M. Nakamura, S. Kinoshita, Keratinocyte growth factor accelerates corneal epithelial wound healing *in vivo*, Invest. Ophthalmol. Vis. Sci. 36 (8) (1995) 1524–1529.
[9] D. Fredj-Reygrobellet, J. Plouet, T. Delayre, C. Baudouin, F. Bourret, P. Lapalus, Effects of aFGF and bFGF on wound healing in rabbit corneas, Curr. Eye Res. 6 (10) (1987) 1205–1209.
[10] P. Rieck, M. Assouline, M. Savoldelli, C. Hartmann, C. Jacob, Y. Pouliquen, Y. Courtois, Recombinant human basic fibroblast growth factor (Rh-bFGF) in three different wound models in rabbits: corneal wound healing effect and pharmacology, Exp. Eye Res. 54 (6) (1992) 987–998.
[11] A. Lambiase, P. Rama, S. Bonini, G. Caprioglio, L. Aloe, Topical treatment with nerve growth factor for corneal neurotrophic ulcers, N. Engl. J. Med. 338 (17) (1998) 1174–1180.
[12] M.C. Manning, K. Patel, R.T. Borchardt, Stability of protein pharmaceuticals, Pharm. Res. 6 (11) (1989) 903–918.
[13] W. Wang, Instability, stabilization, and formulation of liquid protein pharmaceuticals, Int. J. Pharm. 185 (2) (1999) 129–188.
[14] S. Frokjaer, D.E. Otzen, Protein drug stability: a formulation challenge, Nat. Rev. Drug Discov. 4 (4) (2005) 298–306.
[15] C.L. Bourlais, L. Acar, H. Zia, P.A. Sado, T. Needham, R. Leverge, Ophthalmic drug delivery systems—recent advances, Prog. Retin. Eye Res. 17 (1) (1998) 33–58.
[16] J.W. Shell, Pharmacokinetics of topically applied ophthalmic drugs, Surv. Ophthalmol. 26 (4) (1982) 207–218.
[17] D.L. MacKeen, Aqueous formulations and ointments, Int. Ophthalmol. Clin. 20 (3) (1980) 79–92.
[18] R. Hardberger, C. Hanna, C.M. Boyd, Effects of drug vehicles on ocular contact time, Arch. Ophthalmol. 93 (1) (1975) 42–45.
[19] R.E. Hardberger, C. Hanna, R. Goodart, Effects of drug vehicles on ocular uptake of tetracycline, Am. J. Ophthalmol. 80 (1) (1975) 133–138.
[20] D.S. Hull, H.F. Edelhauser, R.A. Hyndiuk, Ocular penetration of prednisolone and the hydrophilic contact lens, Arch. Ophthalmol. 92 (5) (1974) 413–416.
[21] J.S. Hillman, J.B. Marsters, A. Broad, Pilocarpine delivery by hydrophilic lens in the management of acute glaucoma, Trans. Ophthalmol. Soc. U. K. 95 (1) (1975) 79–84.
[22] S.M. Podos, B. Becker, C. Asseff, J. Hartstein, Pilocarpine therapy with soft contact lenses, Am. J. Ophthalmol. 73 (3) (1972) 336–341.
[23] M. Busin, M. Spitznas, Sustained gentamicin release by presoaked medicated bandage contact lenses, Ophthalmology 95 (6) (1988) 796–798.
[24] M.L. Friedberg, U. Pleyer, B.J. Mondino, Device drug delivery to the eye. Collagen shields, iontophoresis, and pumps, Ophthalmology 98 (5) (1991) 725–732.
[25] D.E. Poland, H.E. Kaufman, Clinical uses of collagen shields, J. Cataract Refract. Surg. 14 (5) (1988) 489–491.
[26] J.V. Aquavella, J.J. Ruffini, J.A. LoCascio, Use of collagen shields as a surgical adjunct, J. Cataract Refract. Surg. 14 (5) (1988) 492–495.
[27] Y. Ikada, Y. Tabata, Protein release from gelatin matrices, Adv. Drug Deliv. Rev. 31 (3) (1998) 287–301.
[28] Y. Tabata, A. Nagano, Y. Ikada, Biodegradation of hydrogel carrier incorporating fibroblast growth factor, Tissue Eng. 5 (2) (1999) 127–138.
[29] Y. Tabata, Y. Ikada, Vascularization effect of basic fibroblast growth factor released from gelatin hydrogels with different biodegradabilities, Biomaterials 20 (22) (1999) 2169–2175.
[30] A. Iwakura, Y. Tabata, T. Koyama, K. Doi, K. Nishimura, K. Kataoka, M. Fujita, M. Komeda, Gelatin sheet incorporating basic fibroblast growth factor enhances sternal healing after harvesting bilateral internal thoracic arteries, J. Thorac. Cardiovasc. Surg. 126 (4) (2003) 1113–1120.
[31] Y. Sakakibara, K. Nishimura, K. Tambara, M. Yamamoto, F. Lu, Y. Tabata, M. Komeda, Prevascularization with gelatin microspheres containing basic fibroblast growth factor enhances the benefits of cardiomyocyte transplantation, J. Thorac. Cardiovasc. Surg. 124 (1) (2002) 50–56.
[32] Y. Tabata, K. Yamada, L. Hong, S. Miyamoto, N. Hashimoto, Y. Ikada, Skull bone regeneration in primates in response to basic fibroblast growth factor, J. Neurosurg. 91 (5) (1999) 851–856.
[33] T. Nakano, K. Kaibara, Y. Tabata, N. Nagata, S. Enomoto, E. Marukawa, Y. Umakoshi, Unique alignment and texture of biological apatite crystallites in typical calcified tissues analyzed by microbeam X-ray diffractometer system, Bone 31 (4) (2002) 479–487.
[34] Y. Kimura, M. Ozeki, T. Inamoto, Y. Tabata, Adipose tissue engineering based on human preadipocytes combined with gelatin microspheres containing basic fibroblast growth factor, Biomaterials 24 (14) (2003) 2513–2521.
[35] Y. Tabata, A. Nagano, M. Muniruzzaman, Y. Ikada, *In vitro* sorption and desorption of basic fibroblast growth factor from biodegradable hydrogels, Biomaterials 19 (19) (1998) 1781–1789.
[36] Y. Fukunaka, K. Iwanaga, K. Morimoto, M. Kakemi, Y. Tabata, Controlled release of plasmid DNA from cationized gelatin hydrogels based on hydrogel degradation, J. Control. Release 80 (1–3) (2002) 333–343.
[37] T. Kushibiki, R. Tomoshige, Y. Fukunaka, M. Kakemi, Y. Tabata, In vivo release and gene expression of plasmid DNA by hydrogels of gelatin with different cationization extents, J. Control. Release 90 (2) (2003) 207–216.
[38] T. Kushibiki, R. Tomoshige, K. Iwanaga, M. Kakemi, Y. Tabata, Controlled release of plasmid DNA from hydrogels prepared from gelatin cationized by different amine compounds, J. Control. Release 112 (2) (2006) 249–256.
[39] S.L. Snyder, P.Z. Sobocinski, An improved 2,4,6-trinitrobenzenesulfonic acid method for the determination of amines, Anal. Biochem. 64 (1) (1975) 284–288.
[40] C.o.M.f.T.P. Gelatin, PAGI (Photographic and Gelatin Industries) METHOD, 2002.
[41] F.C. Greenwood, W.M. Hunter, J.S. Glover, The preparation of I-131-labelled human growth hormone of high specific radioactivity, Biochem. J. 89 (1963) 114–123.
[42] A.E. Bolton, W.M. Hunter, The labelling of proteins to high specific radioactivities by conjugation to a 125I-containing acylating agent, Biochem. J. 133 (3) (1973) 529–539.
[43] Y. Ohashi, M. Motokura, Y. Kinoshita, T. Mano, H. Watanabe, S. Kinoshita, R. Manabe, K. Oshiden, C. Yanaihara, Presence of epidermal growth factor in human tears, Invest. Ophthalmol. Vis. Sci. 30 (8) (1989) 1879–1882.
[44] G.B. van Setten, T. Tervo, L. Viinikka, J. Perheentupa, A. Tarkkanen, Epidermal growth factor in human tear fluid: a minireview, Int. Ophthalmol. 15 (6) (1991) 359–362.
[45] W.D. Mathers, M. Sherman, A. Fryczkowski, J.V. Jester, Dose-dependent effects of epidermal growth factor on corneal wound healing, Invest. Ophthalmol. Vis. Sci. 30 (11) (1989) 2403–2406.
[46] H. Sheardown, C. Wedge, L. Chou, R. Apel, D.S. Rootman, Y.L. Cheng, Continuous epidermal growth factor delivery in corneal epithelial wound healing, Invest. Ophthalmol. Vis. Sci. 34 (13) (1993) 3593–3600.
[47] H. Sheardown, H. Clark, C. Wedge, R. Apel, D. Rootman, Y.L. Cheng, A semi-solid drug delivery system for epidermal growth factor in corneal epithelial wound healing, Curr. Eye Res. 16 (3) (1997) 183–190.
[48] O.D. Jimmy, D. Bartlett, Clinical Ocular Pharmacology, Butterworth Publishers, 1984.
[49] J. Lee, Formulation development of epidermal growth factor, Pharmazie 57 (12) (2002) 787–790.
[50] Y. Zhang, G.I. Liou, A.K. Gulati, R.A. Akhtar, Expression of phosphatidylinositol 3-kinase during EGF-stimulated wound repair in rabbit corneal epithelium, Invest. Ophthalmol. Vis. Sci. 40 (12) (1999) 2819–2826.
[51] B. Gonul, D. Erdogan, C. Ozogul, M. Koz, A. Babul, N. Celebi, Effect of EGF dosage forms on alkali burned corneal wound healing of mice, Burns 21 (1) (1995) 7–10.
[52] B.E. Magun, S.R. Planck, L.M. Matrisian, J.S. Finch, Binding, internalization and intracellular processing of 125I-epidermal growth factor purified by isoelectric focusing, Biochem. Biophys. Res. Commun. 108 (1) (1982) 299–306.
[53] E.Y. Kim, Z.G. Gao, J.S. Park, H. Li, K. Han, rhEGF/HP-beta-CD complex in poloxamer gel for ophthalmic delivery, Int. J. Pharm. 233 (1–2) (2002) 159–167.
[54] K. Watanabe, S. Nakagawa, T. Nishida, Stimulatory effects of fibronectin and EGF on migration of corneal epithelial cells, Invest. Ophthalmol. Vis. Sci. 28 (2) (1987) 205–211.